# Crawling chytrid fungi implicate actin regulators WASP and SCAR in an ancient mode of cell motility

Running title: An ancient mode of motility

**Authors:** Lillian K. Fritz-Laylin,[a] Samuel J. Lord,[a] and R. Dyche Mullins[a,1]

[a] Department of Cellular and Molecular Pharmacology, Howard Hughes Medical Institute, University of California, San Francisco CA 94158, USA.

[1] Corresponding author:
Department of Cellular and Molecular Pharmacology
Howard Hughes Medical Institute
University of California, San Francisco
Genentech Hall, Room N312, Box 2200
600 16th Street
San Francisco, CA 94158
Phone number: 415-502-4838
Email: dyche@mullinslab.ucsf.edu

# Abstract

Diverse eukaryotic cells crawl through complex environments using distinct modes of migration. To understand the underlying mechanisms and their evolutionary relationships, we must define each mode, and identify its phenotypic and molecular markers. Here, we focus on a widely dispersed migration mode characterized by dynamic, actin-filled pseudopods that we call "*α*-motility." Mining genomic data revealed a clear trend: only organisms with both WASP and SCAR/WAVE—activators of branched actin assembly—make pseudopods. While SCAR has been shown to drive pseudopod formation, WASP's role in this process is murky. We hypothesize that these genes together represent a genetic signature of *α*-motility, and are used for pseudopod formation. WASP depletion from human neutrophils confirms that both proteins are involved in explosive actin polymerization, pseudopod formation, and cell migration, and colocalize to dynamic signaling structures. Moreover, retention of WASP together with SCAR correctly predicts *α*-motility in disease-causing chytrid fungi, which we show crawl at >30 μm/min with actin-filled pseudopods. By focusing on one migration mode in many eukaryotes, we identified a genetic marker of *α*-motility and evidence for a widely distributed mode of cell crawling with a single evolutionary origin.

# Introduction

Eukaryotic cells move using several distinct modes of locomotion, including crawling and flagella-driven swimming. The stereotyped architecture of flagella and the conservation of their protein components render the evolutionary conservation of cell swimming relatively transparent. In contrast, “crawling motility” is a collection of processes whose functional and evolutionary relationships are not well understood (Lämmermann and Sixt, 2009; Paluch and Raz, 2013; Rodriguez et al., 2005). Some crawling cells require dedicated adhesion molecules to make specific, high-affinity contacts with their surroundings, while other cells rely on weaker, nonspecific interactions. Crawling cells also employ different mechanisms to advance their leading edge, either assembling polymerized actin networks to push the plasma membrane forward, or detaching the membrane from the underlying cytoskeleton to form a rapidly expanding bleb. Furthermore, some cell types have been shown to use contractile forces to generate forward movement (Bergert et al., 2012; Lämmermann et al., 2008; Liu et al., 2015). Different cells can also employ different sets of molecules to drive similar modes of crawling. In an extreme example, nematode sperm have evolved a method of crawling in which polymer assembly advances the leading-edge membrane but, in these cells, the force-generating polymer networks are composed of “major sperm protein” rather than actin. Given this variety of crawling behaviors, it is clear that one cannot simply assume that the underlying molecular mechanisms are the same.

The best understood mode of crawling is the slow (1-10 μm/hour) creeping of adherent animal cells, including fibroblasts and epithelial cells (Petrie and Yamada, 2015). These cells move by extending across a surface a sheet-like protrusion called a lamellipodium while gripping substrate molecules using integrins, often clustered into large focal adhesions. Although clinically and physiologically important, this form of adhesion-based crawling is unique to the animal lineage, and largely restricted to molecular “highways” formed by the extracellular matrix.

In contrast, many motile cells—including free-living amoebae and human immune cells—make three-dimensional, actin-filled pseudopods and navigate complex environments at speeds exceeding 20 μm/min (100-1000× faster than creeping fibroblasts) without forming specific molecular adhesions (Buenemann et al., 2010; Butler et al., 2010). Although this mode of fast cell crawling has been called “amoeboid motility,” this term is also used to describe a range of behaviors, including cell motility that relies on membrane blebs rather than actin-filled pseudopods (Lämmermann and Sixt, 2009).

To narrow our mechanistic focus we use the term “*α*-motility” specifically to describe cell crawling that is characterized by: (i) highly dynamic three-dimensional pseudopods at the leading edge filled with branched-actin networks assembled by the Arp2/3 complex; (ii) fast migration, typically on the order of tens of μm/min; and (iii) the absence of specific, high-affinity adhesions to the extracellular environment. This independence from specific molecular adhesions separates *α*-motility from the adhesion-based motility of fibroblasts and epithelial cells. Furthermore, the use of pseudopods discriminates it

from the fast bleb-based motility adopted by fibroblasts in environments that preclude adhesion formation (Liu et al., 2015; Ruprecht et al., 2015). Some organisms using *α*-motility may also employ additional methods of generating forward movement, such as contractility, retrograde flow, and/or blebbing (Bergert et al., 2012; Lämmermann et al., 2008; Yoshida and Soldati, 2006), but here we focus on a single phenotype readily observable in diverse species, including non-model organisms.

Organisms with cells capable of *α*-motility appear throughout the eukaryotic tree, and we hypothesize that this form of locomotion reflects a single, discrete process that arose early in eukaryotic evolution and has since been conserved. If this hypothesis is correct, then elements of this ancient process—specific molecules and mechanisms—should be conserved and still associated with cell crawling in distantly related organisms that employ *α*-motility. Such molecular remnants would help to unravel the evolutionary history of cell locomotion, and might enable us to predict the existence of specific modes of motility in unexplored species. Identifying genes associated with a process such as *α*-motility is not trivial because the core machinery driving pseudopod formation (e.g. actin and the Arp2/3 complex) is shared with other cellular activities, including some types of endocytosis (Winter et al., 1997). We therefore turned our attention to upstream regulators of actin assembly. WASP and SCAR (also known as WAVE) are widely conserved “nucleation promoting factors” that stimulate branched actin network assembly by the Arp2/3 complex in response to various upstream cellular signals (Koronakis et al., 2011; Moreau et al., 2000; Rohatgi et al., 1999) and promote different levels of Arp2/3 activity (Zalevsky et al., 2001). The broad phylogenetic distributions of WASP and SCAR gene families suggest that both genes are ancient and likely to have been present in the eukaryotic ancestor (Kollmar et al., 2012; Veltman and Insall, 2010), making them appealing candidates for genetic markers of *α*-motility.

SCAR plays a major role in the formation of lamellipodia required for slow, adhesion-dependent migration of fibroblasts (Miki et al., 1998; Steffen et al., 2004) as well as pseudopods at the leading edge of fast-moving amoebae and neutrophils (Veltman et al., 2012; Weiner et al., 2006). In contrast, the involvement of WASP genes—particularly the two mammalian homologs WASP and N-WASP—in cell crawling is less clear, perhaps due to confusion between adhesion-based cell migration and *α*-motility. N-WASP is ubiquitously expressed in mammals, and is dispensable for lamellipodia or filopodia formation by adherent fibroblasts (Lommel et al., 2001; Sarmiento et al., 2008; Snapper et al., 2001), which has lead many researchers to discount a role for any WASP protein in protrusions or motility (Small and Rottner, 2010). Mammalian WASP, on the other hand, is expressed only in blood cells, where it has been shown to be involved in migration and pseudopod formation (Badolato et al., 1998; Burns et al., 2001; Ishihara et al., 2012; G. E. Jones et al., 2002; R. A. Jones et al., 2013; Shi et al., 2009). Recent work has demonstrated that, despite having similar domain organization, the proteins must have distinct biological functions because N-WASP cannot compensate for the migration defect that results from loss of WASP expression in T-cells (Jain and Thanabalu, 2015).The use of WASP by blood cells, the only cells in the body known to build three-dimensional pseudopods, may therefore reflect unique requirements for *α*-motility. Further evidence of this has come from the handful of

papers studying WASP in non-mammallian cells that also point to a role of WASP in cell migration (Veltman et al., 2012; Zhu et al., 2016). (See also Table S1 for an annotated bibliography of 29 papers on WASP and N-WASP relating to cell migration, summarized above.)

To understand the regulation of the actin cytoskeleton during pseudopod formation, we exploited the diversity of organisms that use *α*-motility: by comparing the genomes of many eukaryotes, we found that organisms with genes encoding *both* WASP and SCAR make pseudopods, and organisms that do not build pseudopods have lost either or both Arp2/3 activator. We validated this molecular signature using a negative test (depleting the protein disrupts pseudopod formation in well-studied cells), as well as a positive test (a new prediction of *α*-motility in a little-studied organism). Differentiating *α*-motility from slow/adhesive cell migration helps clarify the confusion over WASP's importance in cell motility, and shifts the major question from whether WASP *or* SCAR is required for motility in a given single cell type, to how WASP and SCAR work *together* to construct and maintain pseudopods in many species. The retention of WASP and SCAR by organisms that form pseudopods represents the first molecular support, to our knowledge, for a single origin of this widespread form of cell motility in an ancestor of extant eukaryotes (see summary **Figure 6**).

# Results

### Evolutionary retention of both WASP and SCAR correlates with pseudopod formation

To trace the evolutionary history of *α*-motility, we first determined which sequenced eukaryotic organisms might employ *α*-motility, combing the literature for references to organisms with cells that form pseudopods. Eukaryotic phyla fall into at least six large clades, and species with sequenced genomes and that form pseudopods can be found in most (**Table 1** and summary **Figure 6**).

On to this map of the phylogenetic distribution of pseudopods, we overlayed the conservation of WASP and SCAR/WAVE genes, using a recently published, manually curated database of nucleation promoting factors from genomes spanning eukaryotic diversity (Kollmar et al., 2012). Multiple analyses indicate that both WASP and SCAR were present in the last common ancestor of eukaryotes (Kollmar et al., 2012; Veltman and Insall, 2010), and therefore argue that a lack of either gene reflects loss during evolution.

To understand whether these gene loss events reveal a significant pattern, we compared the conservation of individual nucleation promoting factors across large evolutionary distances with the ability to assemble pseudopods. We observed a nearly perfect correlation between the conservation of WASP and SCAR and pseudopod formation (**Table 1** and summary **Figure 6**); the only exceptions from this correlation were two little-studied species of chytrid fungi.

For example, *no* plant cells build pseudopods and *no* sequenced plant genomes contain a WASP ortholog. Similarly, multicellular fungi—the dikarya—lack SCAR and are also not known to build pseudopods. Conversely, *almost* all sequenced genomes of Amoebozoan species (including dictyostelids) encode orthologs of WASP and SCAR, and *almost* all move with the help dynamic, actin-rich pseudopods. A interesting example is the amoeba *Entamoeba histolytica*, which forms Arp2/3-dependent phagocytic "food cups" to engulf bacteria (Babuta et al., 2015), but moves using blebs (Maugis et al., 2010), and also lacks genes encoding both WASP and SCAR. We were unable to find a single example of an organism lacking either WASP or SCAR that is capable of constructing motile, actin-rich pseudopods. We did, however, find two little-studied species of chytrid fungi that had retained both nucleation promoting factors, but are not known for *α*-motility, *Allomyces macrogynus* and *Batrachochytrium dendrobatidis.*

We took a two-pronged approach to testing our hypothesis that retention of WASP together with SCAR serves as a molecular signature of pseudopod formation. First, we took the more traditional approach and confirmed that both genes are involved in pseudopod formation in mammalian cells. We followed this with an evolution-based approach by verifying the ability of this molecular signature to predict the capacity for pseudopod formation in chytrid fungi.

**WASP and SCAR localize to the same dynamic arcs within pseudopods of human neutrophils**

Our evolutionary evidence indicates that WASP and SCAR may *both* be required to build pseudopods. To test this hypothesis directly, we turned to human cell lines capable of forming pseudopods. HL-60 cells are derived from an acute myeloid leukemia (Collins et al., 1977) and retain many features of hematopoietic cells, including expression of hematopoietic WASP and the capacity to differentiate into fast-migrating neutrophils with dynamic pseudopods (Collins et al., 1978).

To follow the dynamics of WASP localization in live cells, we created an HL-60 line stably expressing full-length WASP fused at the N-terminus to the red florescent protein TagRFP-T. By confocal fluorescence microscopy, TagRFP-WASP concentrates in two distinct locations within migrating HL-60 cells: punctate foci distributed throughout the cell and a broad zone near the leading edge (**Figure S1A**).

Others have shown that the SCAR regulatory complex localizes to fast-moving, anterograde **"**waves" that break against the leading edge of actively migrating HL-60 cells (Weiner et al., 2007). This localization pattern is most easily observed using total internal reflection fluorescence (TIRF) microscopy, which illuminates a ~100 nm thick region of the cell near the ventral surface (Axelrod, 1981). Using TIRF microscopy on rapidly migrating HL-60 cells, we observed that TagRFP-WASP concentrates near the leading edge in linear arcs that move in an anterograde direction, similar to previously observed patterns of the SCAR regulatory complex (Weiner et al., 2007).

To see whether WASP and the SCAR travel together in the same waves, we introduced TagRFP-WASP into cells expressing YFP-Hem1, a core component of the SCAR regulatory complex (Weiner et al., 2007). TIRF microscopy of these cells revealed that WASP and the regulatory SCAR complex move together in the same dynamic, linear arcs (**Figure 1A-B, Figure S1B,** and **Video 1**). Interestingly, however, the localization patterns of the two are not identical, an observation confirmed by quantifying WASP and SCAR localization across the leading edge (**Figure S1C**). Spinning disk confocal microscopy indicates that WASP and SCAR colocalize throughout the growing pseudopods, not only at the ventral surface (**Figure 1C**). Within the resolution limits of our imaging, the localization patterns move together, with neither protein consistently leading the other (**Figure S1B** and **Video 1**). This dynamic localization pattern suggests that both WASP and SCAR activate the Arp2/3 complex in leading-edge pseudopods, promoting assembly of the branched actin networks required for membrane protrusion.

**WASP participates in pseudopod assembly in neutrophils**

To investigate whether WASP is involved in pseudopod assembly, we generated anti-WASP small hairpin RNAs (shRNAs), expression of which results in a >90% reduction of WASP protein by HL-60 cells (**Figure 2A**). We next examined whether WASP-depleted (WASP-KD) cells can form pseudopods. In a gradient of chemoattractant (the peptide fMet-Leu-Phe), wildtype HL-60 cells become strongly polarized with broad, actin-rich pseudopods used to rapidly move toward the source of chemoattractant (**Figure 2B** and **Video 2**). Compared to control, 50% fewer WASP-KD cells formed pseudopods (**Figure 2B–C**). Despite numerous attempts, we never succeeded in developing WASP-KD cell lines in which this phenotype was 100% penetrant. Although this might reflect the function of residual WASP protein, it is also consistent with the fact that WASP knockout mice show only a partial defect in neutrophil migration *in vivo* (Snapper et al., 2005).

In addition to the defect in pseudopod formation, approximately 20% of WASP-KD cells form large protrusions that taper to a point, reminiscent of a rhinoceros horn (**Figure 2B**, **D**, **Figure S2**, and **Video 2** WASP-KD cells 11, 32, 33, 39 and 42, for example). To verify its specificity, we rescued this “rhino” phenotype by expressing a functional WASP containing three silent mutations in the sequence targeted by to the shRNA (**Figure 2E**). Additionally, a second shRNA that targets a separate region of the WASP gene results in a significantly smaller effect on both WASP expression and the number of cells with the rhino phenotype (not shown). Immunofluorescence combined with phalloidin staining of polymerized actin revealed that the aberrant rhino protrusions contain actin filaments but lack microtubules (**Figure 2D**). The expression of a probe specific for polymerized actin (mCherry fused to calponin homology domain of Utrophin, Utr261 (Burkel et al., 2007)) revealed a highly dynamic and, surprisingly, hollow actin filament network inside the protrusions (**Figure S2**). This distribution—enriched near the membrane but depleted from the core of the protrusion—is more reminiscent of cortical actin networks than of filopodia, which are packed tight with actin bundles (Tilney et al., 1973).

Because some WASP family proteins contribute to endocytosis (Benesch et al., 2005; Merrifield et al., 2004; Naqvi et al., 1998), we investigated whether the defects in WASP-KD cells were caused by reduction of endocytosis. In undifferentiated HL-60s, we observed no difference in transferrin receptor endocytosis and recycling between WASP-KD and control cells (**Figure S3E**). After differentiation into cells capable of making pseudopods, WASP-KD HL-60s actually showed increased internalization, recycling, and surface receptor densities compared to control cells (**Figure S3B–D**). Therefore, we cannot attribute the WASP-KD phenotypes simply to a curtailment of endocytosis activity.

**WASP-depleted neutrophils polymerize less actin in response to chemoattractant**

Addition of chemoattractant to non-polarized (quiescent) HL-60 cells induces a burst of actin polymerization that drives polarization and pseudopod formation, nearly doubling the cell's polymerized actin content within 30 seconds of stimulation. This response is already known to depend on the activity of the SCAR regulatory complex (Weiner et al., 2006). To determine what role WASP might play in this explosive actin assembly, we synchronized pseudopod formation by stimulating populations of quiescent HL-60s with fMLP, fixed and stained the cells with phalloidin at different time points, and analyzed total polymerized actin content in each cell by confocal microscopy and fluorescence-activated cell sorting (FACS) (**Figure 2F–G**). In the absence of chemoattractant, the amount of polymerized actin in quiescent WASP-KD cells is roughly equal to that in control cells. However, as reported for SCAR-depleted cells (Weiner et al., 2006), WASP-KD cells have greatly reduced actin polymerization at both short (30 seconds) and long times (3 min) following stimulation. This reduced actin polymerization indicates that WASP, like SCAR, is central to the explosive actin polymerization required for cell polarization and subsequent pseudopod formation.

**WASP depletion impairs neutrophil motility**

To determine the effect of WASP depletion on cell locomotion, we imaged HL-60 cells migrating through a chemoattractant gradient in a 5 μm tall glass chamber (Millius and Weiner, 2010). Tracking individual cells revealed a severe migration defect in WASP-KD cells (reported mean ± standard deviation of three biological replicates): while control cells move at 12 ± 0.8 μm/min, WASP-KD cells average 5.5 ± 1.5 μm/min, and cells with rhino protrusions are almost completely immotile moving at 1.7 ± 0.4 μm/min **(Figure 3A–B** and **Video 2**). We did not observe an effect of WASP depletion on directional persistence (**Figure 3C**).

Because the chamber we used to measure directional migration is not pre-coated with fibronectin (or any other specific molecule), we doubt this migration defect is due to an integrin-mediated adhesion defect. We confirmed this by directly testing adhesion to fibronectin-coated surfaces found no significant difference between WASP-KD and control cells (**Figure S3A**). We conclude that HL-60 cells use WASP, along with SCAR (Weiner et al., 2006), for normal pseudopod formation and efficient *α*-motility.

**WASP and SCAR genes predict pseudopod formation by chytrid fungi**

The only potential exceptions to the tight correlation between actin-rich pseudopods and the genomic retention of WASP and SCAR were two deeply branching species of fungi, the chytrids *Allomyces macrogynus* and *Batrachochytrium dendrobatidis* (*Bd*). These chytrid species contain genes encoding both WASP and SCAR, but have not been reported in the literature to migrate using pseudopods. We were, however, able to find references to pseudopod formation by unsequenced infectious species related to *A. macrogynus* (*Catenaria anguillulae*), which may employ these structures for motility across the surface of its target host (Deacon, 1997; Gleason and Lilje, 2009). However, because chytrid fungi are not a monophyletic group, but rather comprise multiple deeply branching clades that are estimated to have diverged around 800 million years ago (Stajich et al., 2009) (James et al., 2006), one cannot assume that distantly related species share this capacity. Therefore, we used *Bd* as a predictive test of our hypothesis that WASP and SCAR genes represent a marker for *α*-motility.

Like other species of chytrid fungi, the lifecycle of *Bd* has two stages: a large (10–40 μm) reproductive zoosporangium, which releases a host of small (3–5 μm), motile, flagellated zoospores (Berger et al., 2005; Longcore et al., 1999). These infectious zoospores can form cysts beneath the skin of an amphibian host that develop into new zoosporangia to complete the life cycle (Berger et al., 2005). We searched for *α*-motility in *Bd* zoospores because, unlike the sessile cyst and zoosporangium, these free-swimming flagellates lack a cell wall and have been reported to assume non-uniform shapes with dense “cytoplasmic extensions” (Longcore et al., 1999).

To restrict the fast-swimming *Bd* zoospores to the imaging plane, we adhered zoospores to Concalavin-A coated glass. In initial experiments, we observed only a small fraction (<1%) of zoospores forming pseudopod-like protrusions. The rarity of pseudopod-forming cells suggested that *α*-motility might only occur during a short phase of the life cycle. We therefore enriched for cells of the same age by washing zoosporangia to remove previously released zoospores and collecting flagellates released during the subsequent two hours.

During the first 6 hours after release from the zoosporangium, ~40% of zoospores create dynamic pseudopod-like protrusions (**Figure 4A–B, Figure S4A**, and **Video 3**) that extend from the cell body at a rate of 25 ± 9 μm/min standard deviation (**Figure 4C**), consistent with speeds expected for pseudopods (Chodniewicz and Zhelev, 2003; Zhelev et al., 2004). Unlike blebs, these cellular protrusions are not spherical but irregularly shaped and amorphous—similar to the actin-rich pseudopods of amoebae and neutrophils.

To ensure that these crawling cells were not contaminating organisms, we obtained independently isolated *Bd* cultures from three different laboratories, and observed similar pseudopods in each.

To better investigate the morphology of these tiny pseudopods, we performed scanning electron microscopy on fixed cells (**Figure 4D** and **S4B**), and observed a similar proportion of flagellated zoospores with one or more thick protrusions. Each protrusion

was about 1 μm long and 1 μm wide, and many appeared to be composed of multiple discrete terraces (**Figure 4D** and **S4B**).

**Chytrid pseudopods contain actin and require Arp2/3 activity**

Using our assay to image chytrid zoospores, we next investigated whether extension of *Bd* pseudopods is driven by assembly of branched actin networks, as in other cells crawling using *α*-motility. We first fixed the cells to preserve the actin cytoskeleton and then stained them with fluorescent phalloidin to reveal a thin shell of cortical actin surrounding the cell body and a dense network of filamentous actin filling the pseudopod (**Figure 4E**). To determine whether assembly of the pseudopodial actin network requires the nucleation and branching activity of the Arp2/3 complex, we incubated zoospores with CK-666, a small molecule that inhibits actin nucleation by mammalian and fungal Arp2/3 complexes (Nolen et al., 2009). Addition of 10 μM of CK-666 reduced the number of cells with active protrusions by nearly 100%, an effect reversed by washing out the drug (**Figure 5A–B**). These experiments reveal that protrusion of *Bd* pseudopods requires Arp2/3-dependent actin assembly.

**Chytrid zoospores use pseudopods for *α*-motility**

Although pseudopod-forming *Bd* cells adhere tightly to glass surfaces coated with Concalavin-A, they were not able to move or swim away from the site of initial attachment, and other coatings did not promote any form of attachment (including collagen, fibronectin, and human keratin, not shown). Several types of animal cells are known to migrate without specific molecular adhesions in confined environments (Lämmermann et al., 2008; Liu et al., 2015; Ruprecht et al., 2015). To test whether *Bd* zoospores might also be capable of migration in confined environments, we inserted cells between uncoated glass coverslips, held apart by 1 μm diameter glass microspheres, and observed rapidly migrating cells (**Figure 5C–D, Video 4**). Obviously migrating cells had an average instantaneous speed of 19 ± 9 μm/min standard deviation, with individual cells averaging speeds over 30 μm/min (**Figure 5E**), consistent with the rates of pseudopod extension described above (**Figure 4C**). The trajectories of these cells appeared fairly straight (**Figure 5D**), with an average directional persistence of 0.61 ± 0.25 standard deviation (**Figure 5F**).

Some pseudopod-forming zoospores retained flagella, while other cells had clearly lost or resorbed their flagella and strongly resembled free-living amoebae (**Figure 5C** and **Videos 3**–**4**). We also observed cells switching from crawling to flagellar motility and vice versa, as well as cells rapidly retracting their flagellar axonemes into the cell body (**Video 5**).

# Discussion

Our results reveal that, across eukaryotic phyla, cells capable of constructing actin-rich pseudopods and performing fast, low-adhesion crawling retain, in addition to the Arp2/3 complex, two distinct activators of its actin nucleation activity: WASP and SCAR/WAVE. Our data is well supported by a recent paper implicating both WASP and SCAR in *C. elegans* neuroblast cell migration (Zhu et al., 2016). In that system, the phenotype of

SCAR mutants is enhanced by loss of WASP, and suggests that both WASP and SCAR is found at the leading edge of migrating neuroblasts *in vivo*. Our model is also consistent with requirements for building protrusions that mediate myoblast cell fusion events during muscle formation: like pseudopods, these protrusions are actin-filled force generating machines, and require WASP and SCAR (Sens et al., 2010).

Organisms without the capacity to crawl using pseudopods turn out to have lost one or both of these nucleation-promoting factors (**Table 1** and **Figure 6**). The presence of genes encoding both WASP and SCAR, therefore, provides a molecular correlate for a suite of behaviors that we call "*α*-motility."

The conservation and phylogeny of WASP and SCAR indicate that both were present in a common ancestor of living eukaryotes (Kollmar et al., 2012; Veltman and Insall, 2010). The power of WASP and SCAR as a genomic marker with the ability to identify cryptic pseudopod-forming organisms, together with cell-biology evidence that both WASP and SCAR are required for *α*-motility in well-studied organisms, argues that this widespread behavior arose from single, and ancient origin. Alternatively, it is possible that *α*-motility did not have a single evolutionary origin, but that scenario would require both WASP and SCAR to be co-opted *together* for pseudopod assembly multiple times during eukaryotic history. Because WASP and SCAR are only two of a large number of Arp2/3 activators (Rottner et al., 2010), we have no reason to believe that motility would repeatedly converge on these two in particular.

Together with the metazoans and a handful of protists, fungi form a major clade known as the "opisthokonts" (**Figure 6**). Our identification of *α*-motility in a fungal species argues that the ancestor of all the opisthokonts was capable of fast, pseudopod-associated crawling and that multicellular fungi represent lineages that have lost *α*-motility (Fritz-Laylin et al., 2010). This loss appears to coincide with the disappearance from multicellular fungi of cell types lacking a cell wall. We suggest that the limitations on pseudopod formation imposed by a rigid cell wall obviated any possible selection pressure to preserve gene networks specific for fast crawling motility and the genes unique to this behavior were lost. The fungi would therefore represent a large eukaryotic lineage from which crawling motility has almost completely disappeared.

Images from earlier studies revealed individual *Bd* zoospores with irregular shapes and "cytoplasmic extensions" (Longcore et al., 1999). Actin-driven pseudopod formation and cell motility, however, was not previously described in *Bd* cells, in part because this species was discovered quite recently(Longcore et al., 1999) and relatively few studies have been devoted to its cell biology. In addition, *Bd* zoospores are quite small (<5 μm) and highly motile so that visualizing their tiny (<1 μm) pseudopods requires physical confinement and high-resolution microscopy. Finally, because crawling motility appears most frequently during a specific stage of the *Bd* life cycle—in zoospores recently released from zoosporangia—synchronization of cell cultures was crucial. These advances not only enabled us to observe *α*-motility, but also revealed *Bd* zoospores retracting their flagella by coiling the entire axoneme into the cell body in less than a

second (**Video 5**), a process that has been observed to take minutes in other chytrid species (Koch, 1968).

The *α*-motility of *Bd* fills an important gap in our understanding of the life cycle of this pathogen. As proposed for other chytrid species (Gleason and Lilje, 2009), *Bd* zoospores may use pseudopods during the initial stages of their interaction with a host: either to move across epithelia or crawl between epithelial cells and invade the underlying stroma. Alternatively, our observation that newly hatched zoospores make more pseudopods suggests that *Bd* may rely on *α*-motility to crawl along or within the epithelial surface to uninfected tissues, or to exit the host.

Imaging chytrid zoospores provided key evidence for the involvement of WASP and SCAR in a conserved mode of cell migration, but further exploration of WASP and SCAR function in *Bd* was hampered by several factors. First, the small size of *Bd* zoospores (<5 μm) poses challenges to live-cell imaging. Second, a lack of genetic tools for this species makes it difficult to fluorescently label or deplete proteins in the cells. Third, the lack of potent and specific chemical inhibitors of WASP and SCAR (Bompard et al., 2008; Guerriero and Weisz, 2007) means that it is currently impossible to disrupt their activity chemically.

Several protein families are known to stimulate nucleation activity of the Arp2/3 complex, including WASP, SCAR, JMY, and WHAMM. A conventional explanation for this multiplicity of nucleation promoting factors is that each one directs construction of branched actin networks with different functions at different locations. The conserved connection between WASP, SCAR, and pseudopod formation, however, suggests that this pair of nucleation promoting factors works together to drive the explosive actin polymerization required for pseudopod assembly during *α*-motility. It is possible that WASP and SCAR act together as a “coincidence detector” that integrates multiple signals and damps formation of spurious pseudopods (Stradal and Scita, 2006). This model is supported by studies of the upstream activators of WASP (Cdc42) and SCAR (Rac) (Koronakis et al., 2011; Lebensohn and Kirschner, 2009; Rohatgi et al., 1999; 2000). Specifically, Srinivasan et al. suggest that Rac mediates a positive feedback loop required for leading-edge formation, but the stability of the resulting protrusion requires Cdc42 (Srinivasan et al., 2003).

This model fits the colocalization of WASP and the SCAR regulatory complex at the leading edge (**Figure 1**) and the observation that, while depleting the SCAR regulatory complex leads to a loss of pseudopods in nearly 100% of cells (Weiner et al., 2006), WASP depletion gives only a partially penetrant phenotype. Although it is possible that this is due to residual WASP protein, this seems an insufficient explanation as WASP knockout mice also show only a partial defect in the gross motility of neutrophils *in vivo* (Snapper et al., 2005). This implies a requirement for SCAR in mammalian cells, with WASP playing a supporting role. However, the two proteins may play opposite roles in *Dictyostelium discoideum,* the only non-metazoan amoeboid organism in which WASP and SCAR have been studied: Myers et al. (Myers et al., 2005) reported that high levels of WASP expression are required for cell polarization and chemotaxis*,* and Veltman et

al. (Veltman et al., 2012) found that WASP partially compensates for a deletion of SCAR, maintaining cell motility. This coincidence detection model may also explain the rhino cell morphology observed in WASP-depleted cells: if the formation of robust pseudopods requires activation of Arp2/3 by both WASP and SCAR, the resulting more sparsely branched actin networks generated by WASP-depleted cells might collapse and coalesce into the observed rhino horn structures.

Our results are also supported by papers showing that blood cells rely on WASP for efficient cell migration (Anderson et al., 2003; Binks et al., 1998; Blundell et al., 2008; Dovas et al., 2009; Kumar et al., 2012; Snapper et al., 2005; Worth et al., 2013; Zhang et al., 2006; Zicha et al., 1998), and others suggesting that WASP plays a direct role in protrusion formation, including pseudopods (Badolato et al., 1998; Burns et al., 2001; Ishihara et al., 2012; G. E. Jones et al., 2002; R. A. Jones et al., 2013; Shi et al., 2009). However, these data have been overshadowed by studies showing that fibroblasts do not require N-WASP for filopodia or sheet-like, surface-adhered lamellipodia (Lommel et al., 2001; Sarmiento et al., 2008; Snapper et al., 2001). Such papers have been cited as proof that all WASP family proteins are dispensable for protrusions in general (Small and Rottner, 2010). Such generalizations depend on two assumptions: that N-WASP and WASP have the same molecular function, and that the adherent motility of fibroblasts and *α*-motility use the same molecular pathways. However, recent molecular replacement studies have shown that WASP and the ubiquitously expressed N-WASP have different functions and cannot compensate for each other (Jain and Thanabalu, 2015). Furthermore, when one considers the large body of mammalian WASP literature in the light of distinct modes of motility, a simple pattern emerges: cell types that do not natively express WASP *do not make pseudopods* (although they may make surface-bound lamellipodia, linear filopodia, or adhesive structures called podosomes); WASP is *only* expressed in blood cells, and these cells use WASP for pseudopod-based migration. (See **Table S1** for an annotated summary of WASP/N-WASP literature.) The predominant view that WASP is not involved in cell migration demonstrates the peril of assuming that insights based on adhesion-dependent cell motility apply to other modes of cell crawling.

In addition to *α*-motility, WASP family proteins have been shown to play roles in other cellular processes, including endocytosis (Benesch et al., 2005; Merrifield et al., 2004; Naqvi et al., 1998). The relationship between cell motility and endocytosis and is complex and not completely understood (Schiefermeier et al., 2011; Traynor and Kay, 2007). Rapid pseudopod extension requires not only a large quantity of actin polymerization (Weiner et al., 2006), but also increases membrane tension (Diz-Muñoz et al., 2016), both of which counteract efficient clathrin- and actin-mediated endocytosis (Boulant et al., 2011). Despite this apparent dichotomy between protrusion formation and endocytosis, both WASP and SCAR protein families have been shown to interact with endocytosis pathways. In adherent *Drosophila* cells, for example, membrane-bound clathrin recruits SCAR and promotes lamellipodia formation without additional endocytic machinery (Gautier et al., 2011), and T-cells lacking WASP exhibit impaired receptor internalization (Badour et al., 2007). Here, we find that WASP-deficient HL-60 cells maintain normal receptor internalization and recycling (**Figure S3E**), until

pseudopod activity is activated by differentiation into neutrophils. After differentiation, in addition to being defective in building pseudopods, WASP-KD cells exhibit increased endocytosis and receptor recycling (**Figure S3B-D**). This is consistent with the idea that actin-mediated endocytosis is more efficient when cells are not making pseudopods.

Although a large number of eukaryotes make pseudopods (**Table 1** and **Figure 6**), only two such lineages are currently molecularly tractable: animals and *Dictyostelium*. Experimental data in both of these lineages confirm that pseudopod formation involves both WASP and SCAR proteins. Taken together, this indicates that while the adhesion-dependent migration used by some animal cell types may require a single Arp2/3 activator (SCAR), the explosive actin polymerization required to build three-dimensional pseudopods involves both SCAR and WASP, and both proteins are conserved together to facilitate this evolutionarily ancient mode of cell motility.

# Materials and Methods

**Antibodies and Western Blotting:** anti-WASP (human) antibody was from Santa Cruz (H-250), as was anti-WAVE2 (C-14), anti-tubulin was from Sigma (DM1A), and anti-actin from Calbiochem (JLA20). Western blotting was conducted using standard protocols and horseradish-peroxidase-conjugated secondary antibodies (Jackson Laboratories).

**Generation of HL-60 cell lines:** HL-60 lines were derived from ATCC #CCL-240, and were grown in medium RPMI 1640 supplemented with 15% FBS, 25 mM Hepes, and 2.0 g/L NaHCO3, and grown at 37C and 5% CO2. WASP-KD was achieved using Sigma's Mission Control shRNA vector (TRCN0000029819), with corresponding control vector expressing anti-GFP shRNA (Catalog# SHC005). Lentivirus was produced in HEK293T grown in 6-well plates and transfected with equal amounts of the lentiviral backbone vector (either protein expression vector derived from pHRSIN-CSGW (Demaison et al., 2002), or shRNA expression vectors described above), pCMV$\Delta$8.91 (encoding essential packaging genes) and pMD2.G (encoding VSV-G gene to pseudotype virus). After 48hr, the supernatant from each well was removed, centrifuged at 14,000 g for 5 min to remove debris and then incubated with ~$1\times10^6$ HL-60 cells suspended in 1 mL complete RPMI for 5-12 hours. Fresh medium was then added and the cells were recovered for 3 days to allow for target protein or shRNA expression. TagRFPt-WASP fusion was cloned by first swapping out eGFP for TagRFP-T (Shaner et al., 2008) in the pHRSIN-CSGW by PCR amplifying TagRFP-T with 5'CCCGGGATCCACCGGTCGCCACCATGGTGTCTAAGGGCGAAGAGCTGATTAAG G3' and 5'GAGTCGCGGCCGCTTTAACTAGTCCCGCTGCCCTTGTACAGCTCGTCCATGCCA TTAAGTTTGTGCCCC3' primers, and cloning the resulting PCR product into pHRSIN-CSGW using NotI and BamHI to produce the pHR-TagRFP-T vector. Then, the WASP open reading frame was PCR amplified from cDNA (NCBI accession BC012738) using 5'GCACTAGTATGAGTGGGGGCCCAATGGGAGGAA3' and 5'AAGCGGCCGCTCAGTCATCCCATTCATCATCTTCATCTTCA3' primers, and cloned

into the pHR-TAGRFP-T backbone using NotI and SpeI to result in a single open reading frame containing TagRFPt, a flexible linker (amino acids GSGTS), followed by full length WASP. The WASP shRNA rescue vector was cloned by inserting a P2A cleavage site (Kim et al., 2011) between the linker and a WASP open reading frame edited with site-directed mutagenesis to contain three silent mutations within the shRNA-targetting region (5'cgagacctctaaacttatcta3' was changed to 5'CGAaACCTCTAAgCTcATCTA3', with silent mutations in lower case). A corresponding control vector was designed to express TagRFPt with the flexible linker, but no portion of WASP. The Hem1-YFP line was previously described (Weiner et al., 2006). shRNA lines were selected by puromycin (1 µg/mL for at least 1 week), and florescent cell lines by FACS. HL-60 cells were differentiated by treatment with 1.3% DMSO for 5 days.

**Cytometry:** Fluorescence-activated cell sorting (FACS) analysis was performed on a FACSCalibur analyzer (Bd), Data were analyzed with FlowJo software (Tree Star) and dead cells were gated out using forward and side scatter for all analyses. A FACS Aria II was used for sorting. All FACS analysis was performed at the Laboratory for Cell Analysis (UCSF).

**Imaging:** EZ-TAXIScan (Effector Cell Institute, Tokyo) analysis of HL-60 cell migration between glass surfaces was conducted as previously described (Millius and Weiner, 2010), and cell migration analyzed using Chemotaxis and Migration Tool (Ibidi). Fixed HL-60 cells were imaged with a 100× 1.40 NA oil Plan Apo objective on a motorized inverted microscope (Nikon Ti-E) equipped with a spinning disk (Yokogawa CSU22) and EMCCD camera (Photometrics Evolve). Live TIRF images were acquired by plating HL-60 cells on coverglass cleaned by a 30 min incubation in 3M NaOH, followed by four washes with PBS, pH 7.2, coated for 30 min with 100 µg/mL bovine fibronectin (Sigma F4759) resuspended in PBS. TIRF microscopy images were acquired on a Nikon TE2000 inverted microscope equipped with a 1.45 NA oil 60× or 100× PlanApo TIRF objective and an EMCCD (Andor iXon+), using previously described imaging conditions (Weiner et al., 2007). Fixed chytrid cells were imaged using an inverted microscope (Nikon Ti-E, Tokyo, Japan) equipped with a spinning-disk confocal system with 33 µm pinholes and a 1.8× tube lens (Spectral Diskovery), a Nikon 60× 1.45 NA Apo TIRF objective, and a CMOS camera (Andor Zyla 4.2). DIC microscopy was performed on an inverted microscope (Nikon Ti-E) with a light-emitting diode illuminator (Sutter TLED) and a Nikon 100× 1.45 NA Apo TIRF objective; images were acquired on a CMOS camera (Andor Zyla 4.2). All microscopy hardware was controlled with Micro-Manager software (Edelstein et al., 2010). Image analysis was performed with the ImageJ bundle Fiji. Three-dimensional reconstructions done with the ClearVolume plugin for Fiji/ImageJ (Royer et al., 2015).

**Quantitation of actin polymerization:** HL-60 cells were depolarized in serum free medium supplemented with 2% low-endotoxin BSA (Sigma) for 1 hour at 37C and 5% CO2 before simulation with 20nM fMLP for the indicated time. Cells were immediately fixed with 4% paraformaldehyde in cytoskeleton buffer on ice for 20 min, stained with PBS supplemented with 2% BSA, 0.1% Triton X-100, and 66 nM Alexaflor-488

conjugated phalloidin (Molecular Probes, catalog # A12379) for 20 min, and washed thrice with PBST before FACS analysis.

**Cell adhesion assay**: Differentiated control and WASP-KD HL-60 cells were each stained with either green or blue acetoxymethyl (AM) ester dyes (CellTrace calcein green and blue, ThermoFisher)) and equal numbers mixed and allowed to attach to fibronectin-coated coverglass-bottomed 96 well plates for 30 min at 37C. One set of wells was gently washed three times with fresh media. 100 random locations within the well were immediately imaged, and the percent remaining cells calculated and normalized to control unwashed wells.

**Transferrin uptake endocytosis assays:** $5\times10^6$ differentiated HL-60 cells were washed twice with ice-cold serum-free growth medium (SF), transferred to 37C for 5 min (to clear surface-bound transferrin), and chilled on ice for 1 min. An equal volume of cold SF supplemented with 100ug/mL Alexa488 conjugated transferrin (McGraw and Subtil, 2001) (Molecular Probes T-13342) was added, and incubated on ice for 10 min. Cells were then washed twice with cold SF medium, transferred to 37C for the indicated time period, washed twice with ice-cold acid buffer (8.76 g NaCl, 9.74 g MES in 900 mL, pH to 4.0, water to 1 L), fixed in 4% paraformaldehyde in 1x PBS for 20 min, and washed twice more with ice-cold PBS before immediate FACS analysis.

**Motility of Chytrid zoospores**: *Batrachochytrium dendrobatidis* strain JEL423 was obtained from the laboratory of Joyce Longcore (University of Maine), and grown in 1% tryptone broth or on agar plates (1% tryptone, 2% agar) at 25C. Before imaging, cultures were synchronized by either three washes in 1% tryptone, and zoospores harvested 2 hours later (for liquid cultures), or flooding agar plates with ~2 mL water (for agar plates), passed through a 40 µm filter (Falcon), and collected by centrifuging at 1200 g for 5 min, and resuspended in Bonner's Salts (BONNER, 1947). Cell motility was imaged by sandwiching cells between a #1.5 glass coverslip and glass slide (cleaned by sonicating in pure water) separated using 1 µm glass microspheres (Bangs Laboratories). Coverslip and glass slide were sonicated in deionized water, and dried. Cells were treated with 10 µM CK-666 (Sigma) while cells were adhered to Concalavin-A coated glass. For visualization of polymerized actin: 400 µL fixation buffer (50 mM cacodylate buffer, pH 7.2) supplemented with 4% gluteraldehyde, was added to 100 µL cells attached to a Concalavin-A coated coverslip, and incubated for 20 min at 4C. Samples were quenched with tetraborohydride, permeabilized with 0.1% Triton X-100, incubated for 20 min with Alexa488-labeled phalloidin (Invitrogen), rinsed 4 times, and imaged as above. Samples for scanning electron microscopy were fixed as above, stained with osmium tetroxide, dehydrated, critical point dried, and Au/Pd sputter coated according to standard protocols and imaged using a Hitachi S-5000 scanning electron microscope in the University of California, Berkeley Electron Microscopy Laboratory.

# Acknowledgements:

We would like to thank Jasmine Pare for help with cell culture and HL-60 cell migration assays, and Joyce Longcore, Jason Stajich, and Erica Rosenblum for strains and

helpful discussions. This work was supported by the National Institute of General Medical Sciences of the National Institutes of Health (R01-GM061010 to R.D.M.), by the Howard Hughes Medical Institute Investigator program (R.D.M.), and by a postdoctoral fellowship from the Helen Hay Whitney Foundation supported by the Howard Hughes Medical Institute (L.K.F.-L.).

# References:

Anderson, S.I., Behrendt, B., Machesky, L.M., Insall, R.H., Nash, G.B., 2003. Linked regulation of motility and integrin function in activated migrating neutrophils revealed by interference in remodelling of the cytoskeleton. Cell Motil. Cytoskeleton 54, 135–146. doi:10.1002/cm.10091

Axelrod, D., 1981. Cell-substrate contacts illuminated by total internal reflection fluorescence. J Cell Biol 89, 141–145.

Babuta, M., Mansuri, M.S., Bhattacharya, S., Bhattacharya, A., 2015. The Entamoeba histolytica, Arp2/3 Complex Is Recruited to Phagocytic Cups through an Atypical Kinase EhAK1. PLoS Pathog. 11, e1005310. doi:10.1371/journal.ppat.1005310

Badolato, R., Sozzani, S., Malacarne, F., Bresciani, S., Fiorini, M., Borsatti, A., Albertini, A., Mantovani, A., Ugazio, A.G., Notarangelo, L.D., 1998. Monocytes from Wiskott-Aldrich patients display reduced chemotaxis and lack of cell polarization in response to monocyte chemoattractant protein-1 and formyl-methionyl-leucyl-phenylalanine. J. Immunol. 161, 1026–1033.

Badour, K., McGavin, M.K.H., Zhang, J., Freeman, S., Vieira, C., Filipp, D., Julius, M., Mills, G.B., Siminovitch, K.A., 2007. Interaction of the Wiskott-Aldrich syndrome protein with sorting nexin 9 is required for CD28 endocytosis and cosignaling in T cells. Proc. Natl. Acad. Sci. U.S.A. 104, 1593–1598. doi:10.1073/pnas.0610543104

Benesch, S., Polo, S., Lai, F.P.L., Anderson, K.I., Stradal, T.E.B., Wehland, J., Rottner, K., 2005. N-WASP deficiency impairs EGF internalization and actin assembly at clathrin-coated pits. J. Cell. Sci. 118, 3103–3115. doi:10.1242/jcs.02444

Berger, L., Hyatt, A.D., Speare, R., Longcore, J.E., 2005. Life cycle stages of the amphibian chytrid Batrachochytrium dendrobatidis. Dis Aquat Organ 68, 51–63. doi:10.3354/dao068051

Bergert, M., Chandradoss, S.D., Desai, R.A., Paluch, E., 2012. Cell mechanics control rapid transitions between blebs and lamellipodia during migration. Proc. Natl. Acad. Sci. U.S.A. 109, 14434–14439. doi:10.1073/pnas.1207968109

Binks, M., Jones, G.E., Brickell, P.M., Kinnon, C., Katz, D.R., Thrasher, A.J., 1998. Intrinsic dendritic cell abnormalities in Wiskott-Aldrich syndrome. Eur. J. Immunol. 28, 3259–3267.

Blundell, M.P., Bouma, G., Calle, Y., Jones, G.E., Kinnon, C., Thrasher, A.J., 2008. Improvement of migratory defects in a murine model of Wiskott-Aldrich syndrome gene therapy. Mol. Ther. 16, 836–844. doi:10.1038/mt.2008.43

Bompard, G., Rabeharivelo, G., Morin, N., 2008. Inhibition of cytokinesis by wiskostatin does not rely on N-WASP/Arp2/3 complex pathway. BMC Cell Biol. 9, 42. doi:10.1186/1471-2121-9-42

Bonner, J.T., 1947. Evidence for the formation of cell aggregates by chemotaxis in the development of the slime mold Dictyostelium discoideum. J. Exp. Zool. 106, 1–26.

Boulant, S., Kural, C., Zeeh, J.-C., Ubelmann, F., Kirchhausen, T., 2011. Actin dynamics counteract membrane tension during clathrin-mediated endocytosis. Nat. Cell Biol. 13, 1124–1131. doi:10.1038/ncb2307

Bowers, B., Korn, E.D., 1968. The fine structure of Acanthamoeba castellanii. I. The trophozoite. J Cell Biol 39, 95–111.

Buenemann, M., Levine, H., Rappel, W.-J., Sander, L.M., 2010. The role of cell

contraction and adhesion in dictyostelium motility. Biophys. J. 99, 50–58. doi:10.1016/j.bpj.2010.03.057

Burkel, B.M., Dassow, von, G., Bement, W.M., 2007. Versatile fluorescent probes for actin filaments based on the actin-binding domain of utrophin. Cell Motil. Cytoskeleton 64, 822–832. doi:10.1002/cm.20226

Burns, S., Thrasher, A.J., Blundell, M.P., Machesky, L., Jones, G.E., 2001. Configuration of human dendritic cell cytoskeleton by Rho GTPases, the WAS protein, and differentiation. Blood 98, 1142–1149.

Butler, K.L., Ambravaneswaran, V., Agrawal, N., Bilodeau, M., Toner, M., Tompkins, R.G., Fagan, S., Irimia, D., 2010. Burn injury reduces neutrophil directional migration speed in microfluidic devices. PLoS ONE 5, e11921. doi:10.1371/journal.pone.0011921

Cavalier-Smith, T., Chao, E.E., 2010. Phylogeny and evolution of apusomonadida (protozoa: apusozoa): new genera and species. Protist 161, 549–576. doi:10.1016/j.protis.2010.04.002

Chernikova, D., Motamedi, S., Csürös, M., Koonin, E.V., Rogozin, I.B., 2011. A late origin of the extant eukaryotic diversity: divergence time estimates using rare genomic changes. Biol. Direct 6, 26. doi:10.1186/1745-6150-6-26

Chodniewicz, D., Zhelev, D.V., 2003. Chemoattractant receptor-stimulated F-actin polymerization in the human neutrophil is signaled by 2 distinct pathways. Blood 101, 1181–1184. doi:10.1182/blood-2002-05-1435

Collins, S.J., Gallo, R.C., Gallagher, R.E., 1977. Continuous growth and differentiation of human myeloid leukaemic cells in suspension culture. Nature 270, 347–349.

Collins, S.J., Ruscetti, F.W., Gallagher, R.E., Gallo, R.C., 1978. Terminal differentiation of human promyelocytic leukemia cells induced by dimethyl sulfoxide and other polar compounds. Proc. Natl. Acad. Sci. U.S.A. 75, 2458–2462.

Dayel, M.J., King, N., 2014. Prey capture and phagocytosis in the choanoflagellate Salpingoeca rosetta. PLoS ONE 9, e95577. doi:10.1371/journal.pone.0095577

Deacon, J.W., Saxena, G., 1997. Orientated zoospore attachment and cyst germination in Catenaria anguillulae, a facultative endoparasite of nematodes. Mycological Research 101, 513–522. doi:10.1017/S0953756296003085

Demaison, C., Parsley, K., Brouns, G., Scherr, M., Battmer, K., Kinnon, C., Grez, M., Thrasher, A.J., 2002. High-level transduction and gene expression in hematopoietic repopulating cells using a human immunodeficiency [correction of imunodeficiency] virus type 1-based lentiviral vector containing an internal spleen focus forming virus promoter. Hum. Gene Ther. 13, 803–813. doi:10.1089/10430340252898984

Diz-Muñoz, A., Thurley, K., Chintamen, S., Altschuler, S.J., Wu, L.F., Fletcher, D.A., Weiner, O.D., 2016. Membrane Tension Acts Through PLD2 and mTORC2 to Limit Actin Network Assembly During Neutrophil Migration. PLoS Biol. 14, e1002474. doi:10.1371/journal.pbio.1002474

Dovas, A., Gevrey, J.-C., Grossi, A., Park, H., Abou-Kheir, W., Cox, D., 2009. Regulation of podosome dynamics by WASp phosphorylation: implication in matrix degradation and chemotaxis in macrophages. J. Cell. Sci. 122, 3873–3882. doi:10.1242/jcs.051755

Edelstein, A., Amodaj, N., Hoover, K., Vale, R., Stuurman, N., 2010. Computer control of microscopes using μManager. Curr Protoc Mol Biol Chapter 14, Unit14.20.

doi:10.1002/0471142727.mb1420s92

Fritz-Laylin, L.K., Prochnik, S.E., Ginger, M.L., Dacks, J.B., Carpenter, M.L., Field, M.C., Kuo, A., Paredez, A., Chapman, J., Pham, J., Shu, S., Neupane, R., Cipriano, M., Mancuso, J., Tu, H., Salamov, A., Lindquist, E., Shapiro, H., Lucas, S., Grigoriev, I.V., Cande, W.Z., Fulton, C., Rokhsar, D.S., Dawson, S.C., 2010. The genome of Naegleria gruberi illuminates early eukaryotic versatility. Cell 140, 631–642. doi:10.1016/j.cell.2010.01.032

Fulton, C., 1970. Amebo-flagellates as research partners: The laboratory biology of *Naegleria* and *Tetramitus*, in: Prescott, D.M. (Ed.), Methods Cell Physiol. pp. 341–476.

Gautier, J.J., Lomakina, M.E., Bouslama-Oueghlani, L., Derivery, E., Beilinson, H., Faigle, W., Loew, D., Louvard, D., Echard, A., Alexandrova, A.Y., Baum, B., Gautreau, A., 2011. Clathrin is required for Scar/Wave-mediated lamellipodium formation. J. Cell. Sci. 124, 3414–3427. doi:10.1242/jcs.081083

Gleason, F.H., Lilje, O., 2009. Structure and function of fungal zoospores: ecological implications. Fungal Ecol 2, 53–59. doi:10.1016/j.funeco.2008.12.002

Guerriero, C.J., Weisz, O.A., 2007. N-WASP inhibitor wiskostatin nonselectively perturbs membrane transport by decreasing cellular ATP levels. Am. J. Physiol., Cell Physiol. 292, C1562–6. doi:10.1152/ajpcell.00426.2006

Hertel, L.A., Bayne, C.J., Loker, E.S., 2002. The symbiont Capsaspora owczarzaki, nov. gen. nov. sp., isolated from three strains of the pulmonate snail Biomphalaria glabrata is related to members of the Mesomycetozoea. Int. J. Parasitol. 32, 1183–1191.

Ishihara, D., Dovas, A., Park, H., Isaac, B.M., Cox, D., 2012. The chemotactic defect in wiskott-Aldrich syndrome macrophages is due to the reduced persistence of directional protrusions. PLoS ONE 7, e30033. doi:10.1371/journal.pone.0030033

Jain, N., Thanabalu, T., 2015. Molecular difference between WASP and N-WASP critical for chemotaxis of T-cells towards SDF-1α. Sci Rep 5, 15031. doi:10.1038/srep15031

James, T.Y., Kauff, F., Schoch, C.L., Matheny, P.B., Hofstetter, V., Cox, C.J., Celio, G., Gueidan, C., Fraker, E., Miadlikowska, J., Lumbsch, H.T., Rauhut, A., Reeb, V., Arnold, A.E., Amtoft, A., Stajich, J.E., Hosaka, K., Sung, G.-H., Johnson, D., O'Rourke, B., Crockett, M., Binder, M., Curtis, J.M., Slot, J.C., Wang, Z., Wilson, A.W., Schüssler, A., Longcore, J.E., O'Donnell, K., Mozley-Standridge, S., Porter, D., Letcher, P.M., Powell, M.J., Taylor, J.W., White, M.M., Griffith, G.W., Davies, D.R., Humber, R.A., Morton, J.B., Sugiyama, J., Rossman, A.Y., Rogers, J.D., Pfister, D.H., Hewitt, D., Hansen, K., Hambleton, S., Shoemaker, R.A., Kohlmeyer, J., Volkmann-Kohlmeyer, B., Spotts, R.A., Serdani, M., Crous, P.W., Hughes, K.W., Matsuura, K., Langer, E., Langer, G., Untereiner, W.A., Lücking, R., Büdel, B., Geiser, D.M., Aptroot, A., Diederich, P., Schmitt, I., Schultz, M., Yahr, R., Hibbett, D.S., Lutzoni, F., McLaughlin, D.J., Spatafora, J.W., Vilgalys, R., 2006. Reconstructing the early evolution of Fungi using a six-gene phylogeny. Nature 443, 818–822. doi:10.1038/nature05110

Jones, G.E., Zicha, D., Dunn, G.A., Blundell, M., Thrasher, A., 2002. Restoration of podosomes and chemotaxis in Wiskott-Aldrich syndrome macrophages following induced expression of WASp. Int. J. Biochem. Cell Biol. 34, 806–815.

Jones, R.A., Feng, Y., Worth, A.J., Thrasher, A.J., Burns, S.O., Martin, P., 2013. Modelling of human Wiskott-Aldrich syndrome protein mutants in zebrafish larvae using in vivo live imaging. J. Cell. Sci. 126, 4077–4084. doi:10.1242/jcs.128728

Kim, J.H., Lee, S.-R., Li, L.-H., Park, H.-J., Park, J.-H., Lee, K.Y., Kim, M.-K., Shin, B.A., Choi, S.-Y., 2011. High cleavage efficiency of a 2A peptide derived from porcine teschovirus-1 in human cell lines, zebrafish and mice. PLoS ONE 6, e18556. doi:10.1371/journal.pone.0018556

Knoll, A.H., 2014. Paleobiological perspectives on early eukaryotic evolution. Cold Spring Harb Perspect Biol 6, a016121–a016121. doi:10.1101/cshperspect.a016121

Koch, W.J., 1968. Studies of the Motile Cells of Chytrids. V. Flagellar Retraction in Posteriorly Uniflagellate Fungi. American Journal of Botany 55, 841. doi:10.2307/2440973

Kollmar, M., D. Lbik, and S. Enge. 2012. Evolution of the eukaryotic ARP2/3 activators of the WASP family: WASP, WAVE, WASH, and WHAMM, and the proposed new family members WAWH and WAML. *BMC Res Notes*. 5:88. doi:10.1186/1756-0500-5-88.

Koronakis, V., Hume, P.J., Humphreys, D., Liu, T., Hørning, O., Jensen, O.N., McGhie, E.J., 2011. WAVE regulatory complex activation by cooperating GTPases Arf and Rac1. Proc. Natl. Acad. Sci. U.S.A. 108, 14449–14454. doi:10.1073/pnas.1107666108

Kumar, S., Xu, J., Perkins, C., Guo, F., Snapper, S., Finkelman, F.D., Zheng, Y., Filippi, M.-D., 2012. Cdc42 regulates neutrophil migration via crosstalk between WASp, CD11b, and microtubules. Blood 120, 3563–3574. doi:10.1182/blood-2012-04-426981

Kusdian, G., Woehle, C., Martin, W.F., Gould, S.B., 2013. The actin-based machinery of Trichomonas vaginalis mediates flagellate-amoeboid transition and migration across host tissue. Cell. Microbiol. 15, 1707–1721. doi:10.1111/cmi.12144

Lämmermann, T., Bader, B.L., Monkley, S.J., Worbs, T., Wedlich-Söldner, R., Hirsch, K., Keller, M., Förster, R., Critchley, D.R., Fässler, R., Sixt, M., 2008. Rapid leukocyte migration by integrin-independent flowing and squeezing. Nature 453, 51–55. doi:10.1038/nature06887

Lämmermann, T., Sixt, M., 2009. Mechanical modes of “amoeboid” cell migration. Curr. Opin. Cell Biol. 21, 636–644. doi:10.1016/j.ceb.2009.05.003

Lebensohn, A.M., Kirschner, M.W., 2009. Activation of the WAVE complex by coincident signals controls actin assembly. Mol. Cell 36, 512–524. doi:10.1016/j.molcel.2009.10.024

Liu, Y.-J., Le Berre, M., Lautenschlaeger, F., Maiuri, P., Callan-Jones, A., Heuzé, M., Takaki, T., Voituriez, R., Piel, M., 2015. Confinement and low adhesion induce fast amoeboid migration of slow mesenchymal cells. Cell 160, 659–672. doi:10.1016/j.cell.2015.01.007

Lommel, S., Benesch, S., Rottner, K., Franz, T., Wehland, J., Kühn, R., 2001. Actin pedestal formation by enteropathogenic Escherichia coli and intracellular motility of Shigella flexneri are abolished in N-WASP-defective cells. EMBO Rep. 2, 850–857. doi:10.1093/embo-reports/kve197

Longcore, J.E., Pessier, A.P., Nichols, D.K., 1999. Batrachochytrium Dendrobatidis gen. et sp. nov., a Chytrid Pathogenic to Amphibians. Mycologia 91, 219–227.

doi:10.2307/3761366
Lopes, C.A.M., Jana, S.C., Cunha-Ferreira, I., Zitouni, S., Bento, I., Duarte, P., Gilberto, S., Freixo, F., Guerrero, A., Francia, M., Lince-Faria, M., Carneiro, J., Bettencourt-Dias, M., 2015. PLK4 trans-Autoactivation Controls Centriole Biogenesis in Space. Dev. Cell 35, 222–235.
Maugis, B., Brugués, J., Nassoy, P., Guillen, N., Sens, P., Amblard, F., 2010. Dynamic instability of the intracellular pressure drives bleb-based motility. J. Cell. Sci. 123, 3884–3892. doi:10.1242/jcs.065672
McGraw, T.E., Subtil, A., 2001. Endocytosis: biochemical analyses. Curr Protoc Cell Biol Chapter 15, Unit 15.3. doi:10.1002/0471143030.cb1503s03
Merrifield, C.J., Qualmann, B., Kessels, M.M., Almers, W., 2004. Neural Wiskott Aldrich Syndrome Protein (N-WASP) and the Arp2/3 complex are recruited to sites of clathrin-mediated endocytosis in cultured fibroblasts. Eur. J. Cell Biol. 83, 13–18. doi:10.1078/0171-9335-00356
Miki, H., Suetsugu, S., Takenawa, T., 1998. WAVE, a novel WASP-family protein involved in actin reorganization induced by Rac. EMBO J. 17, 6932–6941. doi:10.1093/emboj/17.23.6932
Millius, A., Weiner, O.D., 2010. Manipulation of neutrophil-like HL-60 cells for the study of directed cell migration. Methods Mol. Biol. 591, 147–158. doi:10.1007/978-1-60761-404-3_9
Moreau, V., Frischknecht, F., Reckmann, I., Vincentelli, R., Rabut, G., Stewart, D., Way, M., 2000. A complex of N-WASP and WIP integrates signalling cascades that lead to actin polymerization. Nat. Cell Biol. 2, 441–448. doi:10.1038/35017080
Myers, S.A., Han, J.W., Lee, Y., Firtel, R.A., Chung, C.Y., 2005. A Dictyostelium homologue of WASP is required for polarized F-actin assembly during chemotaxis. Mol. Biol. Cell 16, 2191–2206. doi:10.1091/mbc.E04-09-0844
Naqvi, S.N., Zahn, R., Mitchell, D.A., Stevenson, B.J., Munn, A.L., 1998. The WASp homologue Las17p functions with the WIP homologue End5p/verprolin and is essential for endocytosis in yeast. Curr. Biol. 8, 959–962.
Nolen, B.J., Tomasevic, N., Russell, A., Pierce, D.W., Jia, Z., McCormick, C.D., Hartman, J., Sakowicz, R., Pollard, T.D., 2009. Characterization of two classes of small molecule inhibitors of Arp2/3 complex. Nature 460, 1031–1034. doi:10.1038/nature08231
Paluch, E.K., Raz, E., 2013. The role and regulation of blebs in cell migration. Curr. Opin. Cell Biol. 25, 582–590. doi:10.1016/j.ceb.2013.05.005
Parfrey, L.W., Lahr, D.J.G., Knoll, A.H., Katz, L.A., 2011. Estimating the timing of early eukaryotic diversification with multigene molecular clocks. Proc. Natl. Acad. Sci. U.S.A. 108, 13624–13629. doi:10.1073/pnas.1110633108
Petrie, R.J., Yamada, K.M., 2015. Fibroblasts Lead the Way: A Unified View of 3D Cell Motility. Trends Cell Biol. 25, 666–674. doi:10.1016/j.tcb.2015.07.013
Ramsey, W.S., 1972. Locomotion of human polymorphonuclear leucocytes. Exp. Cell Res. 72, 489–501.
Rodriguez, M.A., LeClaire, L.L., Roberts, T.M., 2005. Preparing to move: assembly of the MSP amoeboid motility apparatus during spermiogenesis in Ascaris. Cell Motil. Cytoskeleton 60, 191–199. doi:10.1002/cm.20058
Rohatgi, R., Ho, H.Y., Kirschner, M.W., 2000. Mechanism of N-WASP activation by

CDC42 and phosphatidylinositol 4, 5-bisphosphate. J Cell Biol 150, 1299–1310.
Rohatgi, R., Ma, L., Miki, H., Lopez, M., Kirchhausen, T., Takenawa, T., Kirschner, M.W., 1999. The interaction between N-WASP and the Arp2/3 complex links Cdc42-dependent signals to actin assembly. Cell 97, 221–231.
Rottner, K., Hänisch, J., Campellone, K.G., 2010. WASH, WHAMM and JMY: regulation of Arp2/3 complex and beyond. Trends Cell Biol. 20, 650–661. doi:10.1016/j.tcb.2010.08.014
Royer, L.A., Weigert, M., Günther, U., Maghelli, N., Jug, F., Sbalzarini, I.F., Myers, E.W., 2015. ClearVolume: open-source live 3D visualization for light-sheet microscopy. Nat. Methods 12, 480–481. doi:10.1038/nmeth.3372
Ruprecht, V., Wieser, S., Callan-Jones, A., Smutny, M., Morita, H., Sako, K., Barone, V., Ritsch-Marte, M., Sixt, M., Voituriez, R., Heisenberg, C.-P., 2015. Cortical contractility triggers a stochastic switch to fast amoeboid cell motility. Cell 160, 673–685. doi:10.1016/j.cell.2015.01.008
Sarmiento, C., Wang, W., Dovas, A., Yamaguchi, H., Sidani, M., El-Sibai, M., Desmarais, V., Holman, H.A., Kitchen, S., Backer, J.M., Alberts, A., Condeelis, J., 2008. WASP family members and formin proteins coordinate regulation of cell protrusions in carcinoma cells. The Journal of Cell Biology 180, 1245–1260. doi:10.1083/jcb.200708123
Schiefermeier, N., Teis, D., Huber, L.A., 2011. Endosomal signaling and cell migration. Curr. Opin. Cell Biol. 23, 615–620. doi:10.1016/j.ceb.2011.04.001
Sens, K.L., Zhang, S., Jin, P., Duan, R., Zhang, G., Luo, F., Parachini, L., Chen, E.H., 2010. An invasive podosome-like structure promotes fusion pore formation during myoblast fusion. The Journal of Cell Biology 191, 1013–1027. doi:10.1083/jcb.201006006
Shaner, N.C., Lin, M.Z., McKeown, M.R., Steinbach, P.A., Hazelwood, K.L., Davidson, M.W., Tsien, R.Y., 2008. Improving the photostability of bright monomeric orange and red fluorescent proteins. Nat. Methods 5, 545–551. doi:10.1038/nmeth.1209
Shi, Y., Dong, B., Miliotis, H., Liu, J., Alberts, A.S., Zhang, J., Siminovitch, K.A., 2009. Src kinase Hck association with the WASp and mDia1 cytoskeletal regulators promotes chemoattractant-induced Hck membrane targeting and activation in neutrophils. Biochem. Cell Biol. 87, 207–216. doi:10.1139/O08-130
Small, J.V., Rottner, K., 2010. Elementary Cellular Processes Driven by Actin Assembly: Lamellipodia and Filopodia, in: Actin-Based Motility. Springer Netherlands, Dordrecht, pp. 3–33. doi:10.1007/978-90-481-9301-1_1
Snapper, S.B., Meelu, P., Nguyen, D., Stockton, B.M., Bozza, P., Alt, F.W., Rosen, F.S., Andrian, von, U.H., Klein, C., 2005. WASP deficiency leads to global defects of directed leukocyte migration in vitro and in vivo. J. Leukoc. Biol. 77, 993–998. doi:10.1189/jlb.0804444
Snapper, S.B., Takeshima, F., Antón, I., Liu, C.H., Thomas, S.M., Nguyen, D., Dudley, D., Fraser, H., Purich, D., Lopez-Ilasaca, M., Klein, C., Davidson, L., Bronson, R., Mulligan, R.C., Southwick, F., Geha, R., Goldberg, M.B., Rosen, F.S., Hartwig, J.H., Alt, F.W., 2001. N-WASP deficiency reveals distinct pathways for cell surface projections and microbial actin-based motility. Nat. Cell Biol. 3, 897–904. doi:10.1038/ncb1001-897
Srinivasan, S., Wang, F., Glavas, S., Ott, A., Hofmann, F., Aktories, K., Kalman, D.,

Bourne, H.R., 2003. Rac and Cdc42 play distinct roles in regulating PI(3,4,5)P3 and polarity during neutrophil chemotaxis. J Cell Biol 160, 375–385. doi:10.1083/jcb.200208179

Stajich, J.E., Berbee, M.L., Blackwell, M., Hibbett, D.S., James, T.Y., Spatafora, J.W., Taylor, J.W., 2009. The fungi. Curr. Biol. 19, R840–5. doi:10.1016/j.cub.2009.07.004

Steffen, A., Rottner, K., Ehinger, J., Innocenti, M., Scita, G., Wehland, J., Stradal, T.E.B., 2004. Sra-1 and Nap1 link Rac to actin assembly driving lamellipodia formation. EMBO J. 23, 749–759. doi:10.1038/sj.emboj.7600084

Stradal, T.E.B., Scita, G., 2006. Protein complexes regulating Arp2/3-mediated actin assembly. Curr. Opin. Cell Biol. 18, 4–10. doi:10.1016/j.ceb.2005.12.003

Tilney, L.G., Hatano, S., Ishikawa, H., Mooseker, M.S., 1973. The polymerization of actin: its role in the generation of the acrosomal process of certain echinoderm sperm. J Cell Biol 59, 109–126.

Traynor, D., Kay, R.R., 2007. Possible roles of the endocytic cycle in cell motility. J. Cell. Sci. 120, 2318–2327. doi:10.1242/jcs.007732

Veltman, D.M., Insall, R.H., 2010. WASP family proteins: their evolution and its physiological implications. Mol. Biol. Cell.

Veltman, D.M., King, J.S., Machesky, L.M., Insall, R.H., 2012. SCAR knockouts in Dictyostelium: WASP assumes SCAR's position and upstream regulators in pseudopods. J Cell Biol 198, 501–508. doi:10.1083/jcb.201205058

Weiner, O.D., Marganski, W.A., Wu, L.F., Altschuler, S.J., Kirschner, M.W., 2007. An actin-based wave generator organizes cell motility. PLoS Biol. 5, e221. doi:10.1371/journal.pbio.0050221

Weiner, O.D., Rentel, M.C., Ott, A., Brown, G.E., Jedrychowski, M., Yaffe, M.B., Gygi, S.P., Cantley, L.C., Bourne, H.R., Kirschner, M.W., 2006. Hem-1 complexes are essential for Rac activation, actin polymerization, and myosin regulation during neutrophil chemotaxis. PLoS Biol. 4, e38. doi:10.1371/journal.pbio.0040038

Winter, D., Podtelejnikov, A.V., Mann, M., Li, R., 1997. The complex containing actin-related proteins Arp2 and Arp3 is required for the motility and integrity of yeast actin patches. Curr. Biol. 7, 519–529.

Worth, A.J.J., Metelo, J., Bouma, G., Moulding, D., Fritzsche, M., Vernay, B., Charras, G., Cory, G.O.C., Thrasher, A.J., Burns, S.O., 2013. Disease-associated missense mutations in the EVH1 domain disrupt intrinsic WASp function causing dysregulated actin dynamics and impaired dendritic cell migration. Blood 121, 72–84. doi:10.1182/blood-2012-01-403857

Yoshida, K., Soldati, T., 2006. Dissection of amoeboid movement into two mechanically distinct modes. J. Cell. Sci. 119, 3833–3844. doi:10.1242/jcs.03152

Zalevsky, J., Lempert, L., Kranitz, H., Mullins, R.D., 2001. Different WASP family proteins stimulate different Arp2/3 complex-dependent actin-nucleating activities. Curr. Biol. 11, 1903–1913.

Zhang, H., Schaff, U.Y., Green, C.E., Chen, H., Sarantos, M.R., Hu, Y., Wara, D., Simon, S.I., Lowell, C.A., 2006. Impaired integrin-dependent function in Wiskott-Aldrich syndrome protein-deficient murine and human neutrophils. Immunity 25, 285–295. doi:10.1016/j.immuni.2006.06.014

Zhelev, D.V., Alteraifi, A.M., Chodniewicz, D., 2004. Controlled pseudopod extension of human neutrophils stimulated with different chemoattractants. Biophys. J. 87, 688–

695. doi:10.1529/biophysj.103.036699
Zhu, Z., Chai, Y., Jiang, Y., Li, W., Hu, H., Li, W., Wu, J.-W., Wang, Z.-X., Huang, S., Ou, G., 2016. Functional Coordination of WAVE and WASP in C. elegans Neuroblast Migration. Dev. Cell 39, 224–238. doi:10.1016/j.devcel.2016.09.029
Zicha, D., Allen, W.E., Brickell, P.M., Kinnon, C., Dunn, G.A., Jones, G.E., Thrasher, A.J., 1998. Chemotaxis of macrophages is abolished in the Wiskott-Aldrich syndrome. Br. J. Haematol. 101, 659–665.

# Figure Captions

**Figure 1: WASP colocalizes with the SCAR complex at the leading edge of neutrophils.**
Microscopy of HL-60 cells expressing TagRFP-WASP and Hem-1-YFP, a component of the SCAR regulatory complex. For all cells, the direction of migration is to the left. **(A)** TIRF images of live HL-60 cells. Top: WASP localization in three sequential time points, overlayed on the far right (0 seconds in red, 20 seconds in green, and 40 seconds in blue). Middle: same sequence of images, but for Hem-1. Bottom: overlay of WASP and Hem-1 at each time point. The plot shows line scans of normalized fluorescence intensity of WASP (red) and Hem-1 (green). The location for generating the line scans is shown in the adjacent image. See also **Video 1**. **(B)** Two additional examples of live HL-60 cells in TIRF and corresponding line scans. **(C)** Spinning disk confocal images of two fixed HL-60 cells, showing an axial slice through the middle of thick pseudopods. The slices shown were taken 3 μm above the coverslip. See also **Figure S1**.

**Figure 2. WASP is crucial for explosive actin polymerization during pseudopod formation of neutrophils.**
**(A)** Western blots showing WASP expression in control HL-60 cells (WT), cells expressing shRNA to WASP and exogenous WASP with three silent mutations in the region corresponding to the shRNA (KD+rescue), or cells expressing anti-WASP shRNA and empty vector rescue control (KD+control). Equal amounts of total protein were loaded in each lane, confirmed using actin as a loading control. **(B)** Brightfield microscopy of control and WASP knockdown cells. **(C)** Knockdown of WASP using shRNA reduces the percentage of cells that have pseudopods. Means and standard deviations of three biological replicates (with >135 cells total) are displayed; p value from two-tailed paired t-test. **(D)** Immunofluorescence of control and WASP-KD HL-60 cells showing microtubules (green, antibody-stained), actin filaments (red, phalloidin-stained), and DNA (blue, DAPI). Note the signature rhino phenotype in the WASP-KD cell. See also **Figure S2**. **(E)** Rescue of rhino protrusion phenotype by expression of shRNA insensitive WASP as described in A. Note: no wildtype cells were observed to exhibit the rhino phenotype. Means and standards deviation of three biological replicates (with >130 cells total) are displayed; p value from two-tailed paired t-test. **(F)** Spinning disk confocal images of polymerized actin of control and WASP-KD HL-60 cells after stimulation for the indicated time with chemoattractant (20 nM fMLP), stained with florescent phalloidin**. (G)** Polymerized actin of control (grey squares) and WASP-KD HL-60 cells (green triangles) after stimulation for the indicated time with chemoattractant, stained with florescent phalloidin, and quantified with FACS. 10,000 cells were counted for each sample, and normalized to time zero for control within each experiment.

**Figure 3. WASP is crucial for neutrophil motility.**
**(A)** Worm plots showing the tracks of cell migrating up a fMLP chemoattractant gradient: control cells (left), WASP-KD cells (right), with cells that exhibit the rhino phenotype in red. Cells were imaged 20 min, and migration paths overlaid, with time zero at (0,0). The endpoint of each cell's path is shown with a dot. See also **Video 2.**

**(B)** Depletion of WASP protein leads to reduced cell speed. The average instantaneous speed for each cell in (A) is plotted as a dot, color-coded by biological replicate to highlight the consistency from experiment to experiment. The average of the three replicates is displayed as a horizontal line; p values from two-tailed paired t-test. (**C**) Reduction of WASP protein leads to no significant change in directional persistence (the ratio of the Euclidean distance to the accumulated distance) of cells tracked in (A).

**Figure 4. Genomic retention of both WASP and SCAR correctly predicts pseudopod formation by the infectious chytrid fungus *B. dendrobatidis*.**
Throughout figure, pseudopods are indicated by brackets and flagella by arrowheads. **(A)** Time lapse showing examples of pseudopods from chytrid cells with (middle) and without a flagellum (middle), or one cell of each (bottom). See also **Video 3**. (**B**) Percentage of cells with pseudopods within first six hours after release from zoosporangia. Mean and standard deviation of four biological replicates (with 3782 cells total) are displayed. (**C**) Pseudopod extension rates. Mean and standard deviation of the combined values from three biological replicates are displayed. **(D)** Scanning electron micrographs of fixed chytrid zoospores. **(E)** Fixed chytrid cells with (top) and without a flagellum (middle and bottom). Staining with fluorescent phalloidin reveals a thin shell of cortical actin surrounding the cell body and a dense network of polymerized actin filling the pseudopods.

**Figure 5. Genomic retention of both WASP and SCAR correctly predicts *α*-motility in the infectious chytrid fungus *B. dendrobatidis*.**
**(A)** Two examples of chytrid cells with pseudopods that lose them when treated with 10 µm CK-666, an inhibitor of Arp2/3 activity. Pseudopods (indicated by brackets) return after drug washout. **(B)** Quantitation of reversible inhibition of pseudopods by CK-666. Only cells that were making pseudopods before treatment and that were not washed away during the experiment were counted. Results from three biological replicates shown; p values from two-tailed paired t-test. **(C)** Example chytrid zoospore without flagellum migrating when confined between 1 µm spaced glass coverslips. **(D)** Worm plots showing the tracks of migrating chytrid zoospores, with migration paths overlaid, with time zero at (0,0). The endpoint of each cell's path is shown with a dot. Only those cells obviously migrating were tracked, and for the duration of their movement. **(E)** Average instantaneous speed of cells tracked in (D). Mean and standard deviation of the combined values from three biological replicates are displayed. **(F)** Directional persistence (the ratio of the Euclidean distance to the accumulated distance) of cells tracked in (D). Mean and standard deviation of the combined values from three biological replicates are displayed.

**Figure 6. Only organisms that make pseudopods retain both WASP and SCAR genes.**
Diagram showing the relationships of extant eukaryotes (based on (Fritz-Laylin et al., 2010)), with presence or absence of SCAR (blue) and WASP (green) genes from complete genome sequences as described (Kollmar et al., 2012). The representative organism whose genome was used for the analysis is listed to the right. For groups with similar morphological and sequence patterns, a single species is used. For example,

there is no known plant species that forms pseudopods or retains the WASP gene, so only a single species is shown (*Arabidopsis thaliana*); similarly, *Aspergillus nidulans* represents all dikarya. See (Kollmar et al., 2012) for additional sequence information. An amoeba glyph indicates organisms that build pseudopods. Outlined rectangles indicate a lack of identifiable gene. See **Table 1** for citations and full species names. *Although we were not able to find a reference to pseudopod formation in *A. macrogynus*, a relative (*Catenaria anguillulae)* does assemble pseudopods used for motility (Gleason and Lilje, 2009). Because of this, and the conservation of both WASP and SCAR in *B. dendrobatidis*, we predict this species is also capable of pseudopod formation. ++These species form pseudopods for feeding, rather than motility. "?" Indicates uncertainty regarding the structure of the protrusions for phagocytosis in *Entamoeba histolytica* (see text). The time of divergence of extant eukaryotic groups has been estimated to be 1.1-2.3 billion years ago (Chernikova et al., 2011) (Knoll, 2014; Parfrey et al., 2011) and has been predicted to have possessed both WASP and SCAR gene families (Kollmar et al., 2012) and therefore may have built pseudopods.

**Figure S1. WASP localizes to pseudopods of migrating neutrophils.**
**(A)** Maximum projection image of localization of TagRFP-WASP and Hem-1-YFP (a member of the SCAR regulatory complex) expressed in differentiated HL-60 cells fixed while migrating on a fibronectin-coated surface. **(B)** Kymographs of pseudopods of two live HL-60 cells, showing colocalization over time of TagRFP-WASP and Hem-1-YFP patterns. Time from left (T=0) to right, and direction from bottom (inside cell) to top (outside cell). See **Video 1** for the cells from which these kymographs were generated. **(C)** Linescans following the contour of the leading edge of cells in Figure 1, showing that TagRFP-WASP (red) partially colocalizes with Hem-1-YFP (green).

**Figure S2. WASP depletion in neutrophils leads to dynamic, hollow rhino protrusions.**
**(A)** Time-lapse microscopy of a live WASP-KD HL-60 cell with aberrant "rhino" protrusions, with polymerized actin visualized using Utrophin261-mCherry. Time is shown in (min : seconds), and an immobile arrowhead highlights protrusion dynamics. **(B)** Isolated three-dimensional reconstructions of spinning disk confocal stacks of HL-60 cells with fluorescent probe specific for polymerized actin (mCherry fused to calponin homology domain of Utrophin, Utr261). The rhino horns are denoted by brackets in the top view. The side views confirm that the rhino horns are hollow with a shell of actin (indicated by arrowheads). **(C)** Cross sections through the rhino horns from panel (B).

**Figure S3. WASP is not required for adhesion or endocytosis by HL-60 cells.**
**(A)** WASP-KD does not significantly reduce the HL-60 cells' ability to adhere to fibronectin-coated surfaces. Bars represent averages from three biological replicates, normalized to control in each experiment; p value from two-tailed paired t-test. **(B)** Steady state endocytosis was measured for WASP-KD (green) and control cells (black) by incubating cells for 10 minutes at 37C with fluorescent transferrin, immediately washing with ice-cold acid buffer (to remove surface-bound transferrin). Cells were then fixed, and endocytosed tranferrin quantified by FACS analysis. Values were normalized to percent control within each experiment. **(C)** Quantitation of actin-mediated

endocytosis and receptor recycling in differentiated (neutrophil-like) control (black circles) and WASP-KD HL-60 cells (green squares). Cells were incubated with florescent transferrin, placed at 37C for the indicated time, washed with ice-cold acid buffer (to remove surface-bound transferrin), and fixed for FACS analysis. Within each experiment, samples for each cell line were normalized to time zero. Averages and standard deviations for three independent experiments are shown. (**D**) Transferrin receptor density was measured by incubating cells at 37C in serum-free medium (to remove surface-bound transferrin), chilling cells and incubating on ice with florescent transferrin. Cells were then washed with PBS to remove unbound transferrin and fixed. Surface-bound transferrin was then quantitated by FACS analysis. Values were normalized to percent control within each experiment. (**E**) Quantitation of actin-mediated endocytosis and receptor recycling in undifferentiated control (black squares) and WASP-KD HL-60 cells (green triangles). Cells were incubated with florescent transferrin, placed at 37C for the indicated time, washed with ice-cold acid buffer (to remove surface-bound transferrin), and fixed for FACS analysis. Within each experiment, samples for each cell line were normalized to time zero. Averages and standard deviations for three independent experiments are shown.

**Figure S4**
**(A)** DIC image of representative field of synchronized *Bd* zoospores. Asterisks are highlighted by cells with obvious pseudopods. Rapidly-swimming flagellate cells are blurred. **(B)** Additional examples of scanning electron micrographs of chytrid zoospores.

# Video Legends

**Video 1.** Five examples of lapse movies showing TIRF microscopy of live differentiated HL-60 neutophil cells expressing Hem-1-YFP (top, and green in overlay) and TagRFP-WASP (middle, and red in overlay). White lines indicate position for kymographs in **Figure S1B**.

**Video 2.** Migration of control differentiated HL-60 neutrophil cells and of differentiated WASP-KD HL-60 cells in 2D environment (EZ-TAXIScan assay). Cells expressing control shRNA migrating in a chemoattractant gradient (source is at top) between two glass surfaces with 5 µm spacing. All cells initially within the field of view were manually tracked, as shown. Images were acquired every 20 seconds and are displayed at 300X speed. Many WASP-KD cells exhibited the rhino phenotype and their motility was effectively abolished (e.g. cells 11, 32, 33, 39 and 42).

**Video 3**. Time lapse movies showing the representative examples of *Bd* chytrid zoospores with pseudopods imaged using DIC microscopy pictured in **Figure 4B**, including a cell with flagella (bottom left), a cell without a flagellum (bottom right), and one cell of each (top).

**Video 4**. Examples of *Bd* chytrid cell crawling between two glass coverslips separated by 1 µm glass beads. See also **Figure 5**.

**Video 5**. Time lapse imaging showing an example of flagellar retraction by *Bd* chytrid zoospores.

# Table 1

WASH, WAVE and WASP gene orthologs for indicated species. Orthologs were identified in (Kollmar et al., 2012), which also provides protein sequences. Example references for observations of pseudopods are given. Cases where genes or reference to cells with active pseudopod were not found are indicated by "n.f."

| Species | Group | WAVE | WASP | Pseudopod reference |
|---|---|---|---|---|
| *H. sapiens* | Animals (opisthokont) | WAVE1, WAVE2, WAVE3 | WASP, N-WASP | (Ramsey, 1972) |
| *M. brevicollis* | Opisthokont | MbWAVE | MbWASP | (Dayel and King, 2014) |
| *C. owczarzaki* | Opisthokont | CoWAVE | CoWASP | (Hertel et al., 2002) |
| *A. nidulans* (Representative dikaryon) | Fungi (opisthokont) | n.f. | EnWASP | n.f. |
| *B. dendrobatidis* | Fungi (opisthokont) | Bad_bWAVE | Bad_bWASP | see Figure 2 |
| *A. macrogynus* | Fungi (opisthokont) | AlmWAVE | AlmWASP_Aalpha, AlmWASP_Abeta, AlmWASP_Balapha, AlmWASPB_beta | n.f. |
| *D. discoideum* | Amoebozoan | SCAR1 | DdWASP | (Lopes et al., 2015) |
| *E. histolytica* | Amoebozoan | n.f. | n.f. | n.f. |
| *A. castellanii* | Amoebozoan | AcWAVE | AcWASP_A, AcWASP_B, AcWASP_C | (Bowers and Korn, 1968) |
| *T. trahens++* | Apusozoa | TctWAVE | TctWASP | (Cavalier-Smith and Chao, 2010) |
| *A. thaliana* | Plant | SCAR1, SCAR2, SCAR3, SCAR4, SCAR-like domain-containing protein | n.f. | n.f. |
| *P. ramorum* | Chromalveolate | n.f. | n.f. | n.f. |
| *B. natans* | Chromalveolate | n.f. | BinWASP_A, BinWASP_B | n.f. |
| *P. faliciparum* | Chromalveolate | n.f. | n.f. | n.f. |
| *T. thermophila* | Chromalveolate | n.f. | TtWASP_A, TtWASP_B | n.f. |
| *E. huxleyi* | Rhizarian | n.f. | *Emh*Wasp | n.f. |
| *N. gruberi* | Heterolobosean | NgWAVE_A, NgWAVE_B | NgWASP_A, NgWASP_B, NgWASP_C, NgWASP_D | (Fulton, 1970) |
| *G. lamblia* | Diplomonad | n.f. | n.f. | n.f. |
| *T. vaginalis* | Parabasalid | Tv_aWAVE_A, Tv_aWAVE_B, Tv_aWAVE_C, Tv_aWAVE_D, Tv_aWAVE_E, Tv_aWAVE_F, Tv_aWAVE_G, Tv_aWAVE_H, Tv_aWAVE_I, Tv_aWAVE_J, Tv_aWAVE_K | Tv_aWasp_A, Tv_aWasp_B | (Kusdian et al., 2013) |

Figure 1: WASP colocalizes with the SCAR complex at the leading edge of neutrophils.

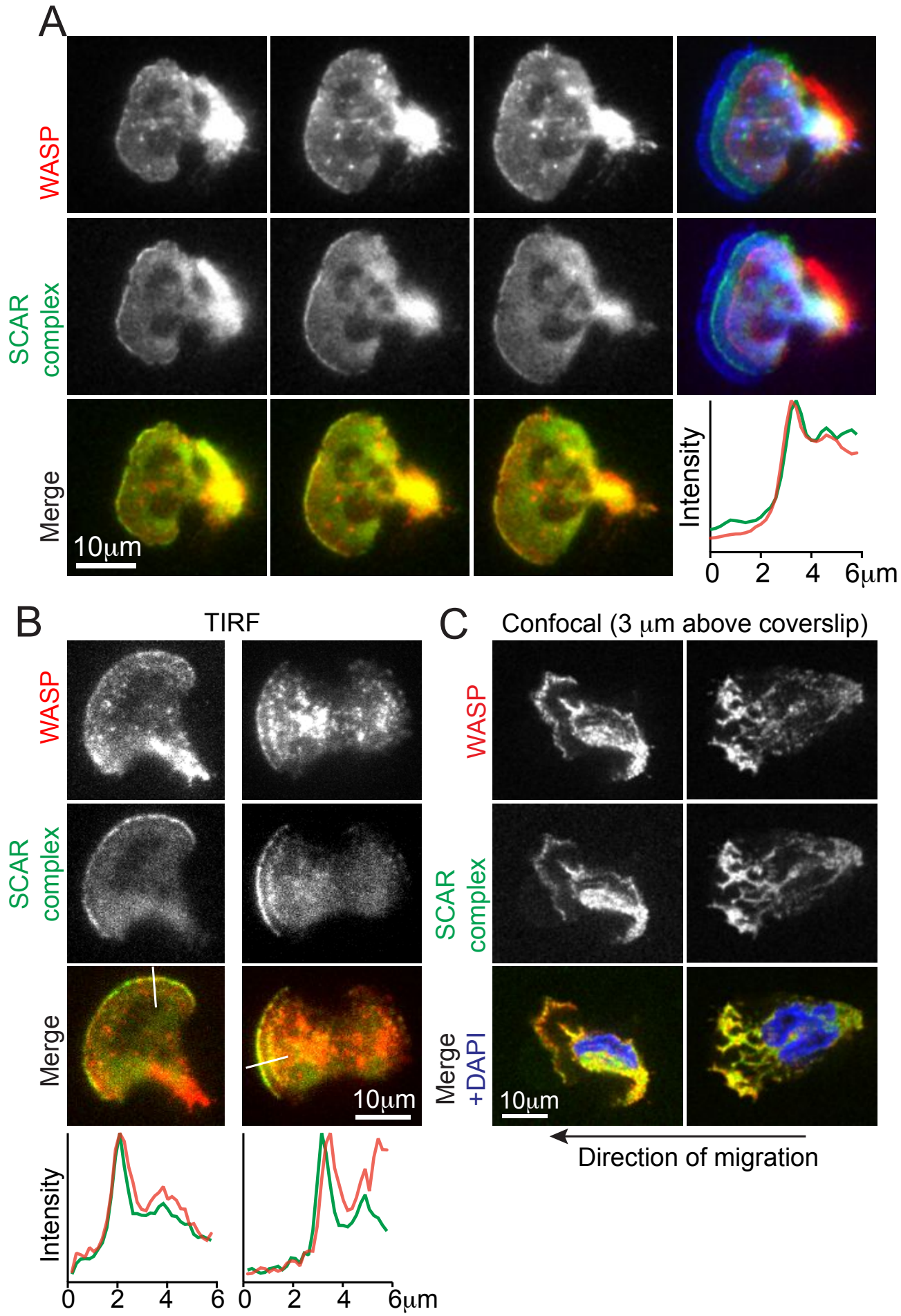

Figure 2. WASP is crucial for explosive actin polymerization during pseudopod formation of neutrophils.

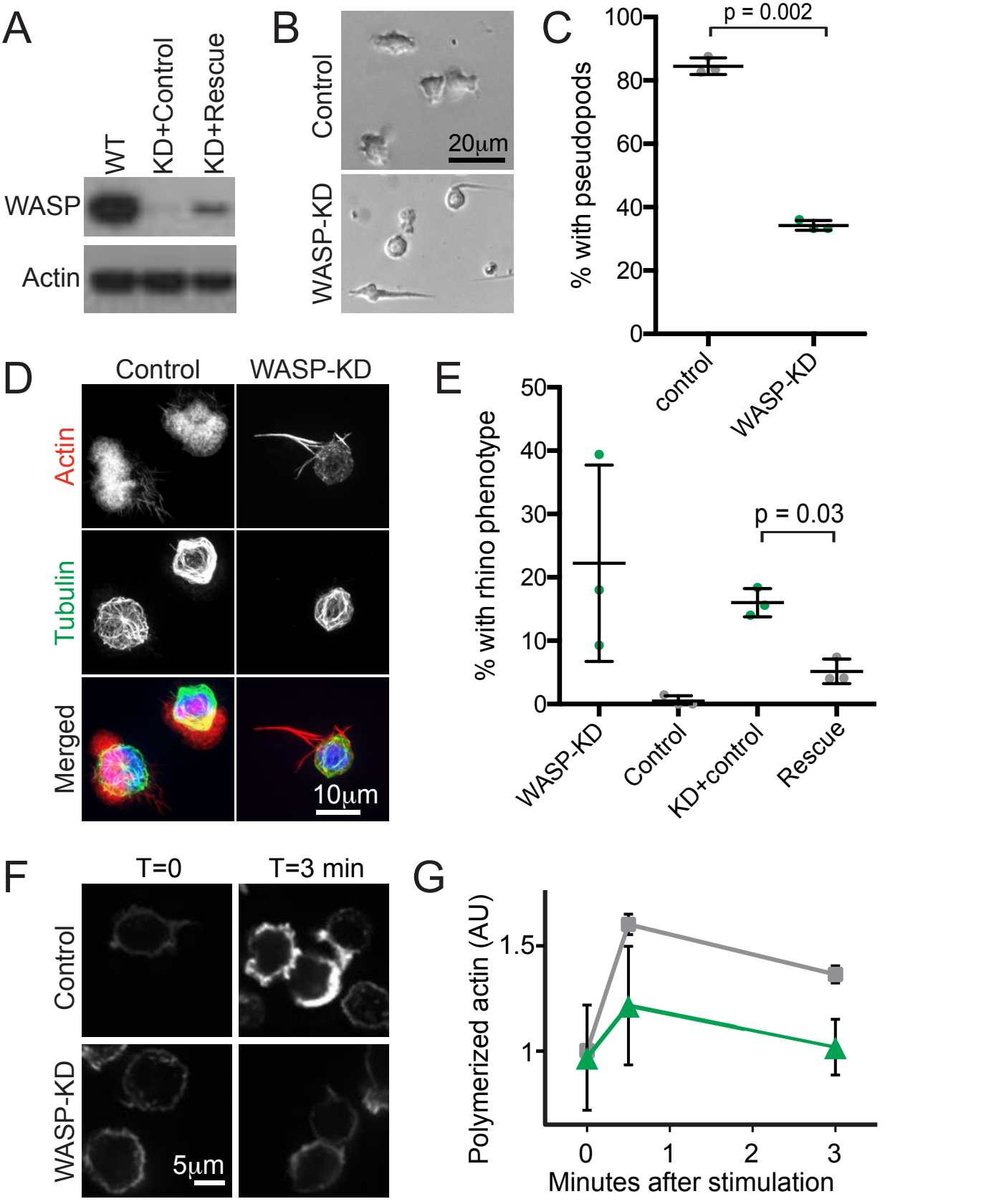

Figure 3. WASP is crucial for neutrophil motility.

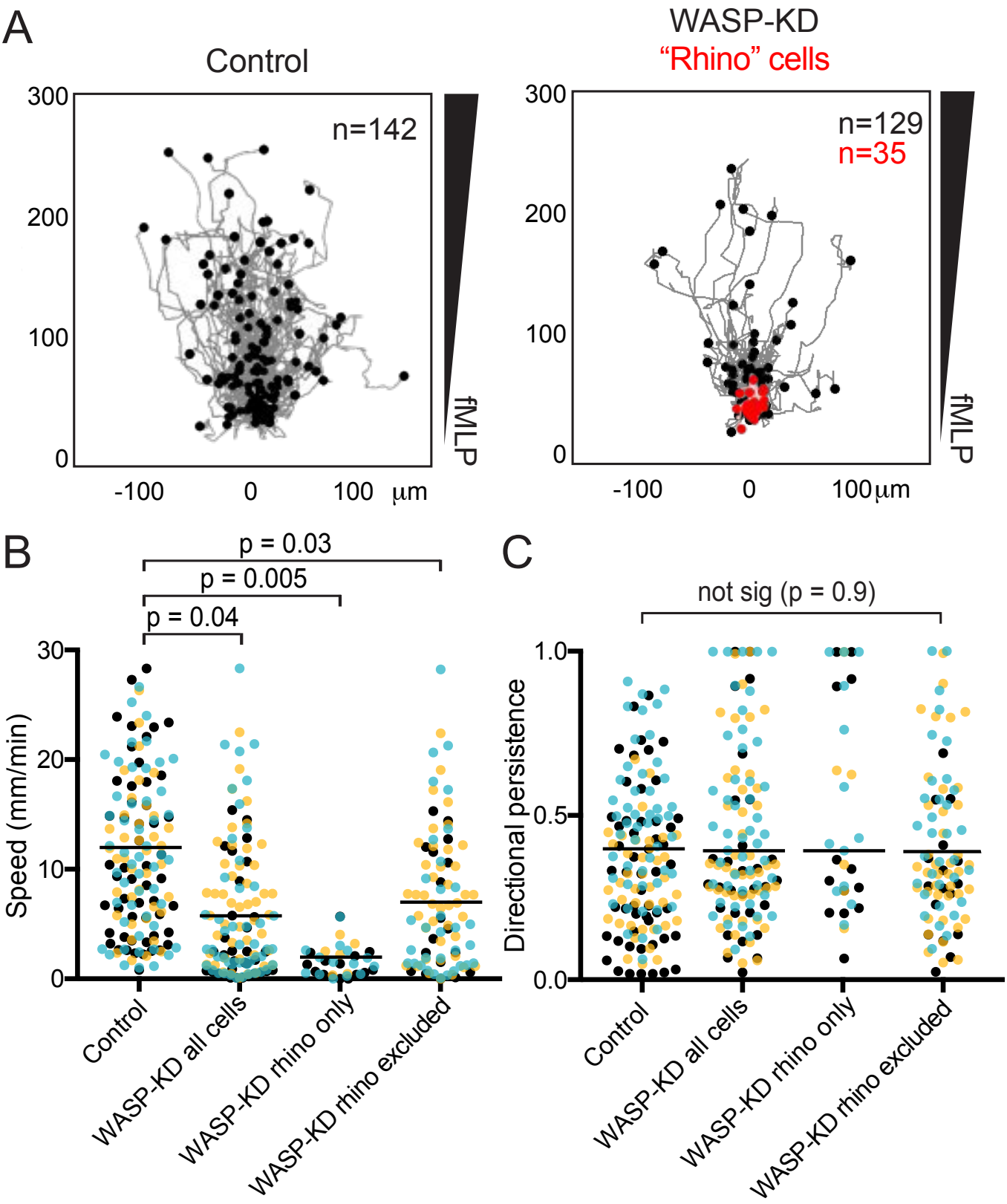

Figure 4. Genomic retention of both WASP and SCAR correctly predicts pseudopod formation by the infectious chytrid fungus *B. dendrobatidis*.

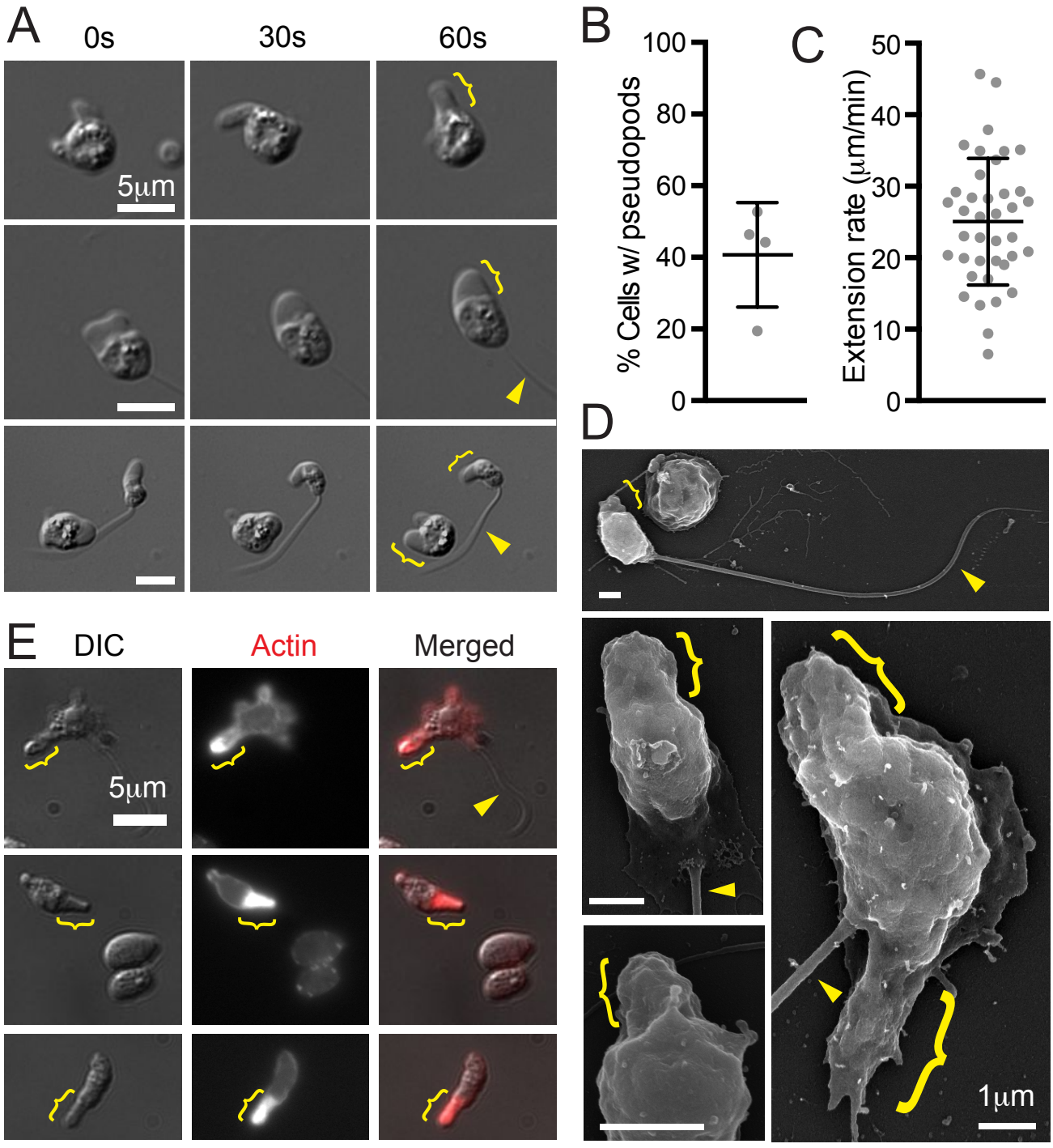

Figure 5. Genomic retention of both WASP and SCAR correctly predicts *α*-motility in the infectious chytrid fungus *B. dendrobatidis*.

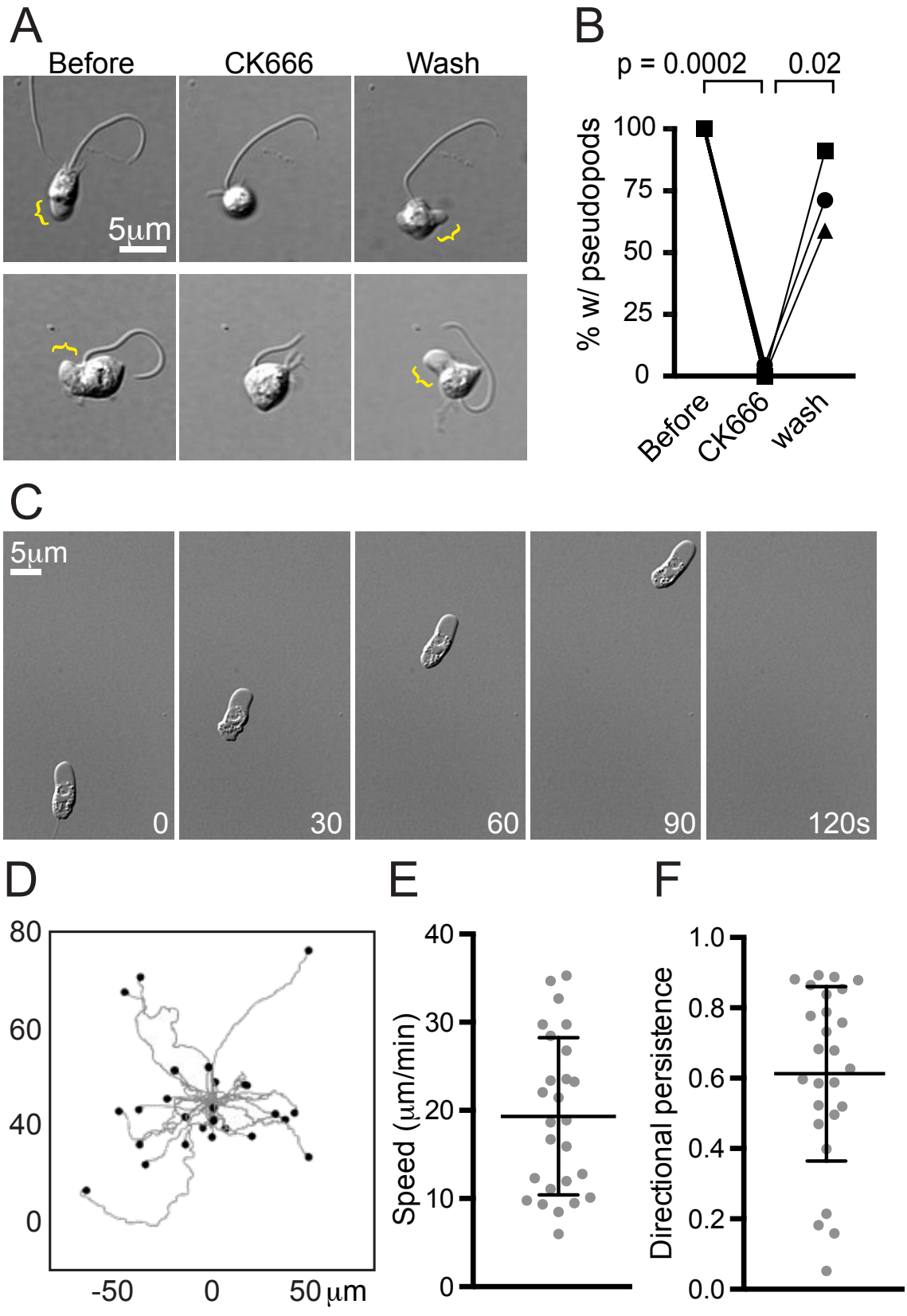

Figure 6. Only organisms that make pseudopods retain both WASP and SCAR genes.

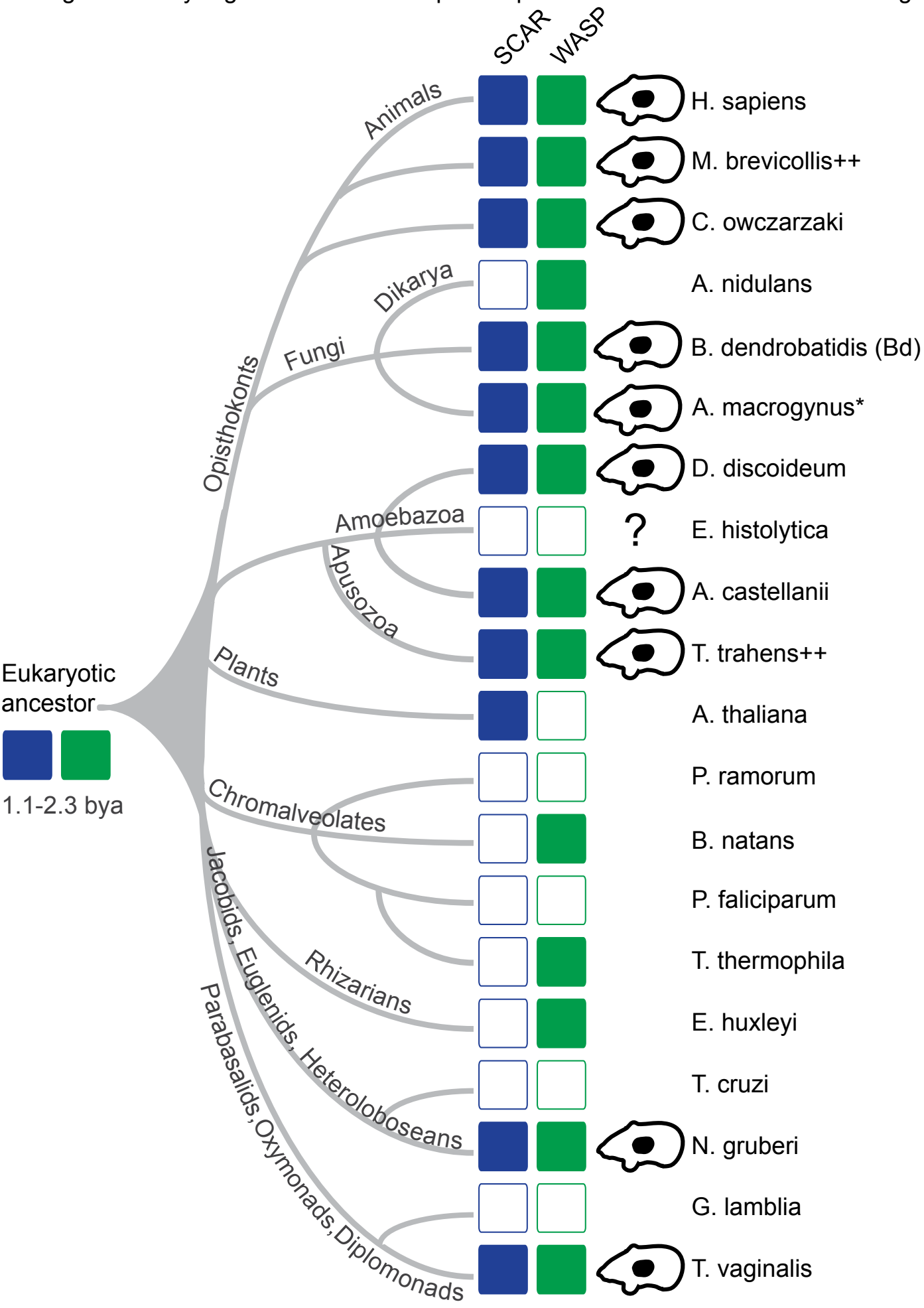

Figure S1: WASP localizes to pseudopods of migrating neutrophils.

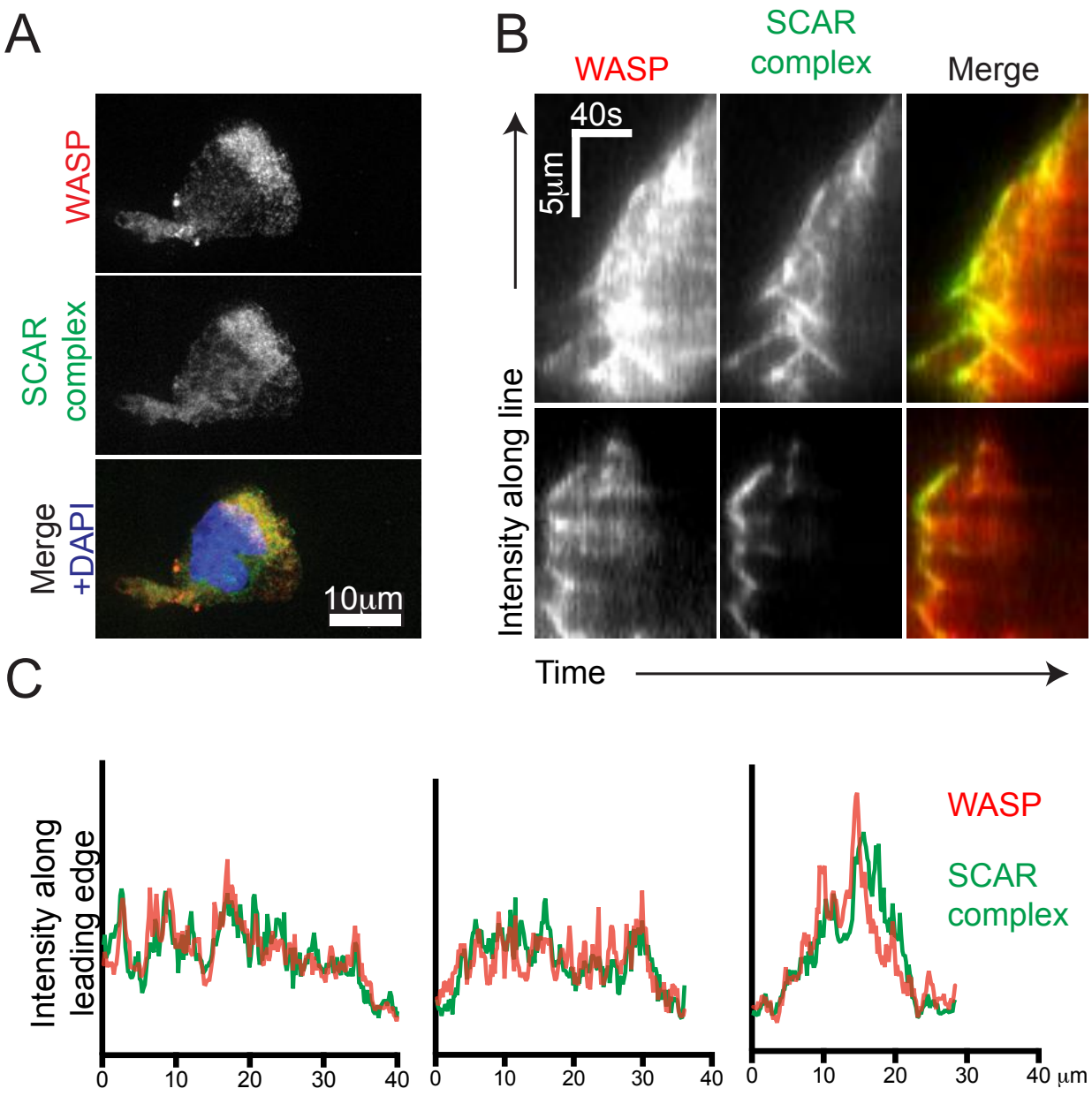

Figure S2. WASP depletion in neutrophils leads to dynamic, hollow “rhino” protrusions.

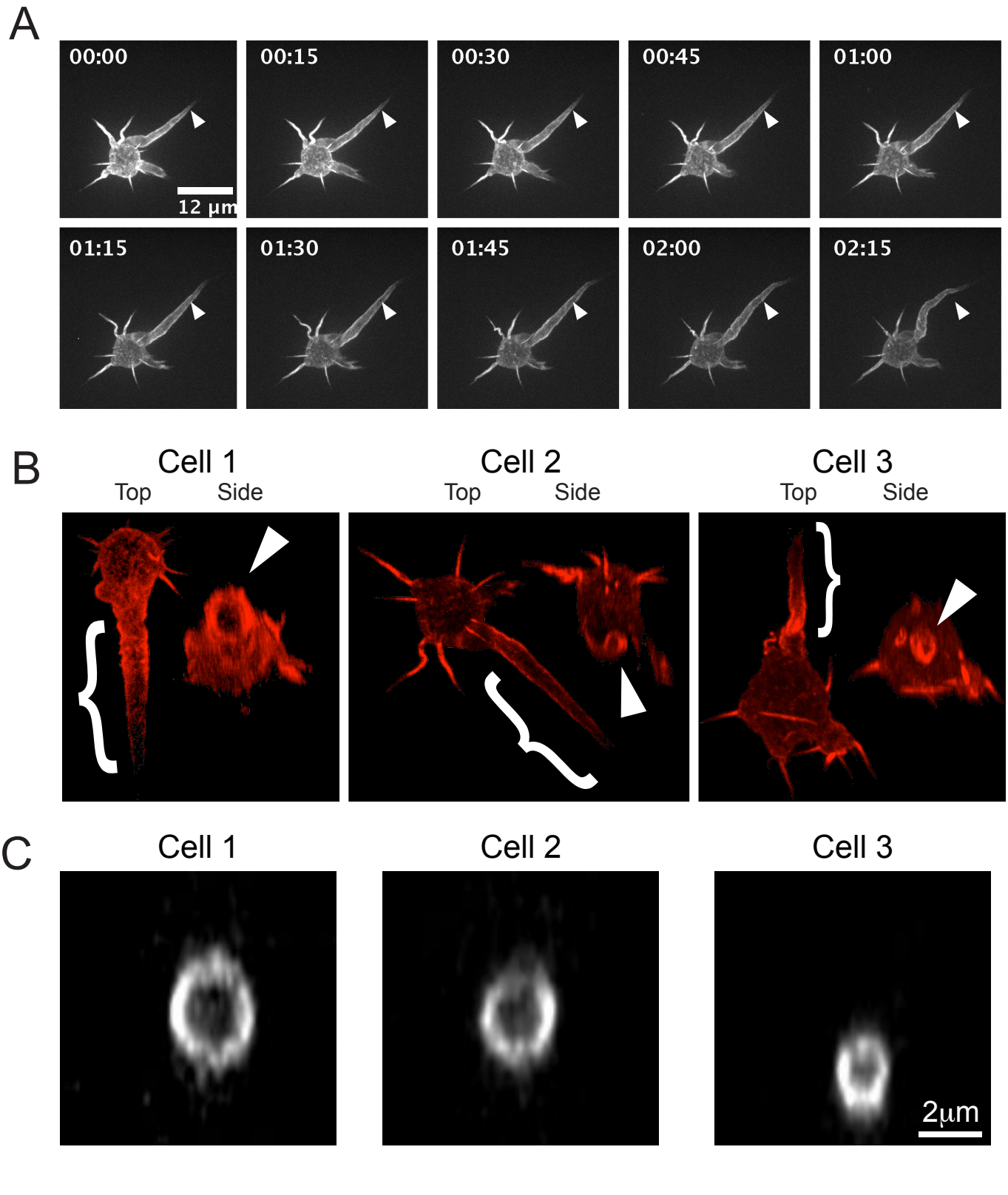

Figure S3. WASP is not required for adhesion or endocytosis by HL-60 cells.

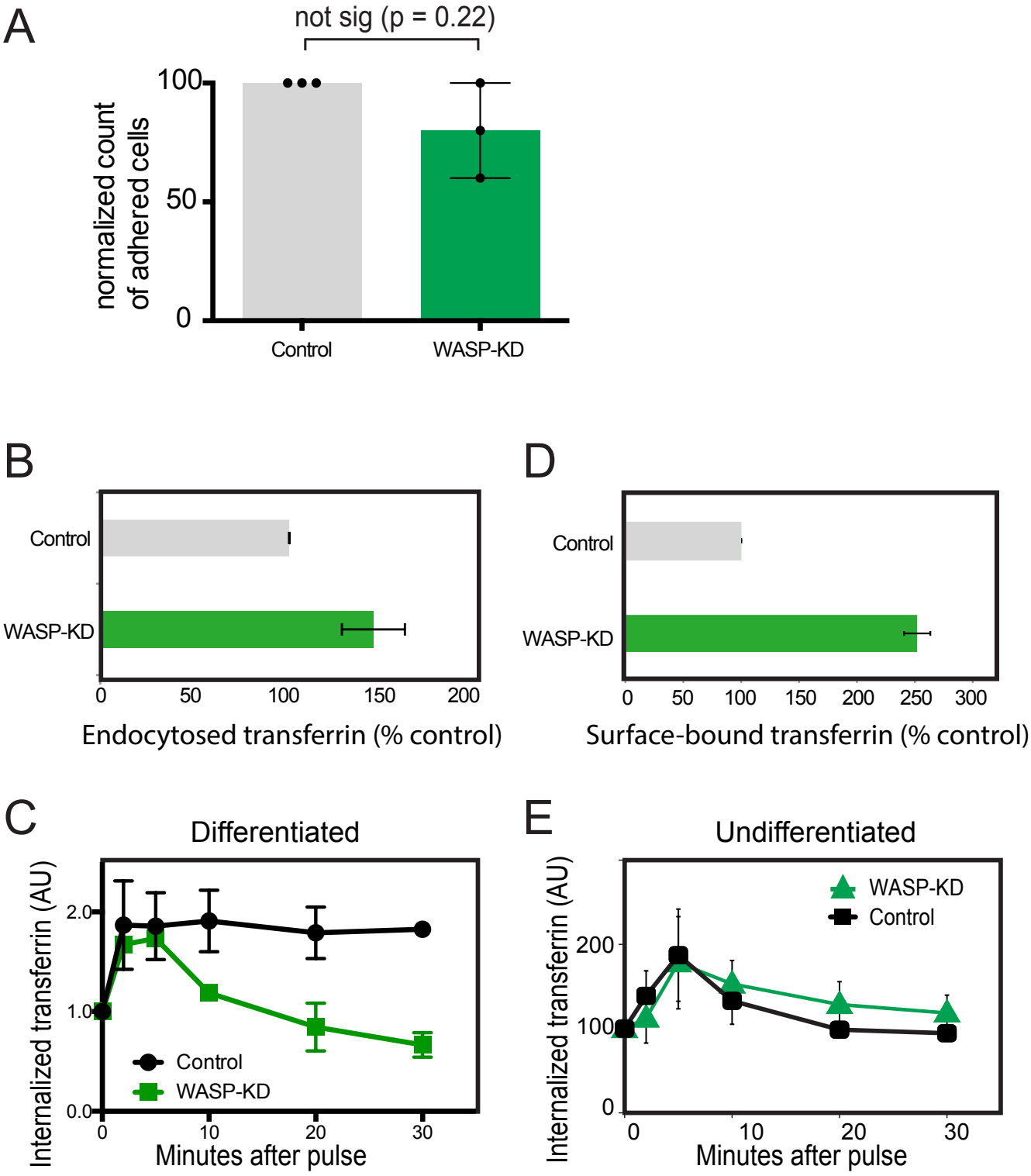

Figure S4

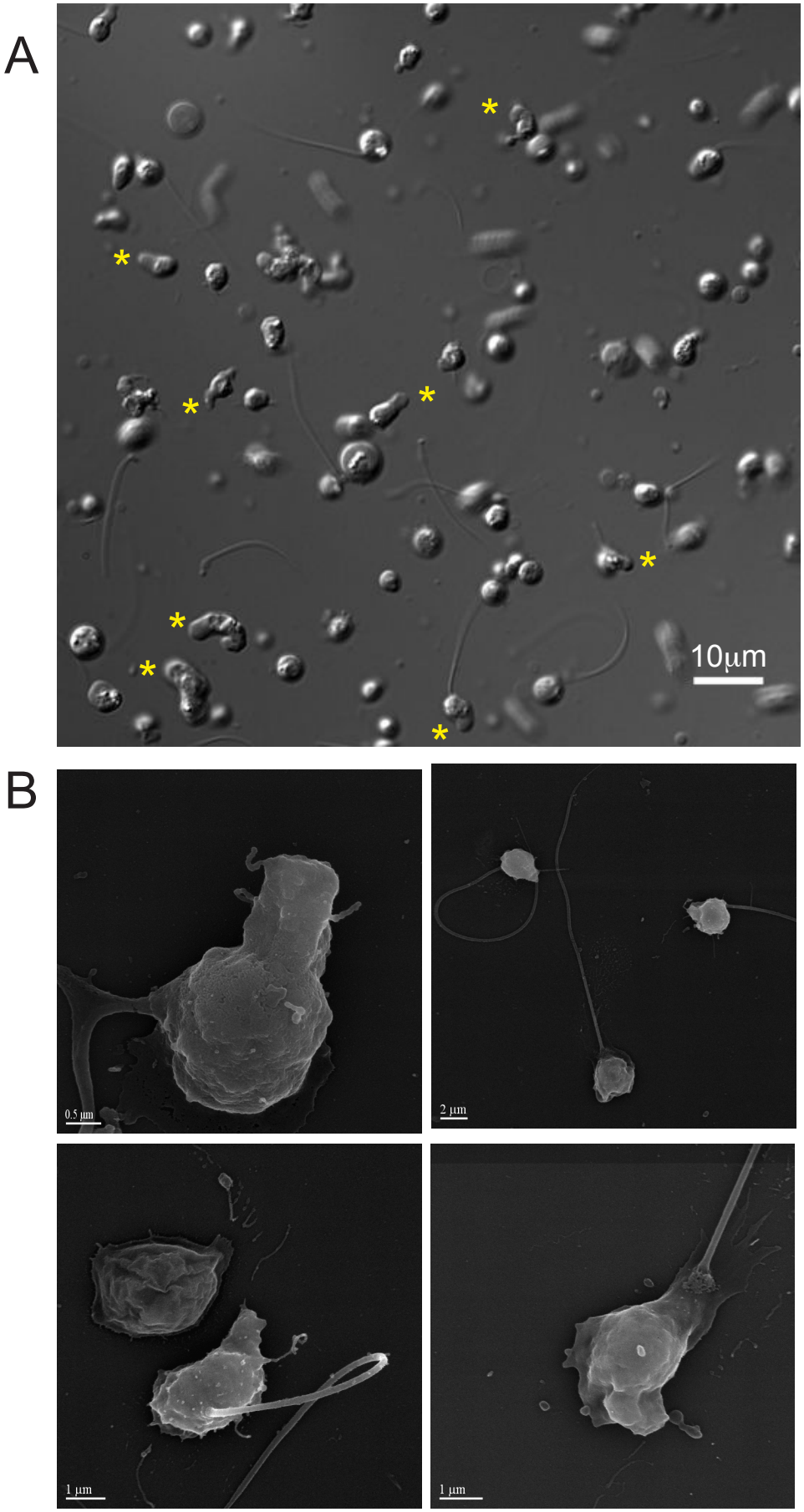

# Table S1

## Part 1: Fast/blood cell (expressing WASP)

| Paper (PMID) | Cell type | Finding |
|---|---|---|
| Jones 2002 (11950596) | Macrophages (from blood of human WAS patients) | Migrating macrophages that lack WASP fail to form actin-rich protrusions. WASP-deficient cells moved aberrantly and did not have directionality toward a chemotractant. See Figure 2. |
| Burns 2001 (11493463) | Dendritic cells (from blood of human WAS patients) | Expressing WASP restores actin- and WASP-filled protrusions. Arp2/3 is also shown to be enriched in the protrusions. “Persistent broad, leading-edge lamellipodia do not form” and translocation is “severely compromised” in WASP-deficient cells. See Figure 5. |
| Badolato 1998 (9670984) | Monocytes (from human WAS patients) | Cells from WAS patients remained rounded upon stimulation with chemotractant and their migration was severely impaired; normal monocytes in their assay showed a polarized actin distribution and readily formed pseudopods |
| Binks 1998 (9808195) | Dendritic cells (from human WAS patients) | Cells from WAS patients were “unable to polarize normally and have severely reduced translocational motility in vitro.” (Although they did still see “ruffles” in the WASP-deficient cells, they did not observe larger lamellar structures.) |
| Zicha 1998 (9674738) | Machrophages and neutrophils (from human WAS patients) | Macrophages from WAS patients had defects in directional chemotaxis, although neutrophils from the same patients were not disrupted. Both mutant and wildtype cells moved at approximately the same speed.<br><br>Notably, the statistical analysis in this paper eliminated any cell that did not reach a certain distance (60 um for neutrophils and 10 um for macrophages), and therefore ignored cells with severely impaired motility. |
| Linder 1999 (10449748) | Macrophages (from human WAS patients) | Cells from WAS patients formed fewer podosomes and filopodia, which were distributed around the entire cell instead of just at the leading edge. |
| Snapper 2005 (15774550) | Neutrophils (WASP-KO mouse) | Defect in chemotaxis in WASP-deficient cells (by 25-50%) |
| Kumar 2012 (22932798) | Neutrophils (WASP-KO mouse) | Cdc42 controls neutrophil chemotaxis and polarity via WASP. “$WASP^{-/-}$ neutrophils have defective chemotaxis and exhibit loss of polarity.” Cells lacking WASP exhibit significantly lower speed (“Sp”) and straightness (“St.”). The authors also report that WASP-deficient cells exhibit a huge increase in the *number* of protrusions, with many smaller protrusions occurring on the sides of cells instead of at the front. |
| Anderson 2003 (12529859) | Neutrophils (blood from healthy humans) | Neutrophils were loaded with purified SCAR or WASP peptides. High concentrations of SCAR severely disrupted motility, and WASP had a smaller effect. |
| Zhang 2006 (16901726) | Neutrophils (WASP-KO mouse) | WASP-deficient cells had impaired adhesion and remain unpolarized, rounded, and without protrusions. Their transendothelial migration was also severely disrupted. |
| Jones 2013 (23868979) | Neutrophils (Zebrafish) | Inside zebrafish embryos, reduced protrusions and cell velocity in cells with UAS-WASP mutant. See Figure 1G. |
| Shi 2009 (19234535) | Neutrophils (WASP-KO | WASP localizes to pseudopods of chemotacting cells. See Figure 1C. |

| | | |
|---|---|---|
| | mouse) | |
| Dovas 2009 (19808890) | Macrophages mouse and human) | Phosphoylation/dephosphoylation of WASP was required for normal podosome formation and turnover and fibronectin matrix degradation. Chemotaxis was impaired by RNAi-reduction of WASP and was rescued by adding WASP, but not by a phosphorylation mutant. |
| Ishihara 2013 (22279563) | Macrophages (WASP-KO mouse) | WASP is responsible for an initial wave of actin polymerization in response to global stimulation with chemotractant. Protrusions from WASP-deficient cells were directional, showing intact directional sensing. However, the protrusions from WASP-deficient cells demonstrated reduced persistence compared to wildtype cells. |
| Myers 2005 (15728724) | Dictyostelium | Cells will reduced levels of WASP exhibit defects in polarized actin assembly, cell migration, and chemotaxis |
| Veltman 2012 (22891261) | Dictyostelium | When SCAR/WAVE is knocked out, WASP assumes the localization and presumably some of the functions of SCAR/WAVE |
| Jain 2015 (26463123) | Jurkat T-cells (human) | Knocking down WASP in Jurkat T-cells slowed motility and abolished directionality. Overexpression of N-WASP in WASP-KD cells restored the migration velocity without correcting the chemotactic defect. However, insertion of a section of the WASP amino acid sequence into N-WASP enabled N-WASP to rescue the chemotactic defect of WASP-KD cells. |
| Worth 2012 (23160469) | Dendritic (WASP-KO mouse) | Cells lacking WASP form multiple unpolarized lamellipodia and exhibit migration defects (in persistence and directionality, although not speed). Expressing exogenous WASP rescues normal protrusions and migration. |
| Blundell 2008 (18388921) | Dendritic (WASP-KO mouse) | Number of podosome protrusions as reduced in WASP-KD cells and could be rescued by transducing with WASP. Speed of WASP-KD cells was drastically reduced compared to wildtype and WASP-rescue cells. |
| Zhu 2016 (27780040) | Neuroblasts (C. Elegans) | Migrating neuroblasts in developing worms use both WASP and SCAR/WAVE. SCAR mutations reduced migration and WASP mutation further impaired motility in SCAR-deficient cells. |

## Part 2: Cells with adhesion-based motility (expressing N-WASP)

| Paper (PMID) | Cells type | Finding |
|---|---|---|
| Misra 2007 (17963692) | Adherent fibroblasts (mouse N-WASP$^{del/del}$ cell line) | N-WASP deletion disrupts adhesion |
| Bryce 2005 (16051170) | Adherent fibrosarcoma cells (human) | N-WASP knockdown by siRNA did not reduce lamellapod formation. By removing an N-WASP activator from cells the lamellipods were not as persistent, cell migration was defective, and fewer adhesions formed |
| DesMarais 2009 (19373774) | Carcinoma cells (rat) | Cells depleted of N-WASP using siRNA show a defect in invadopodium-based chemotaxis |
| Sarmiento 2008 (18362183) | Carcinoma cells (rat) | siRNA WAVE depletion inhibited lamellipod formation to a greater degree than N-WASP. Depleting both resulted in aberrant jagged protrusion |
| Bensenor 2007 (17264147) | Slowly crawling MDBK (bovine) | N-WASP, Arp2/3, and actin all localize to protrusions. N-WASP is required for FGF2-stimulated migration |
| Lommel 2001 (11559594) | Adherent fibroblasts (mouse N-WASP$^{flox/flox}$) | Adherent cells lacking N-WASP still form filopodia |
| Tang 2013 | Carcinoma cells | “N-WASP has a crucial proinvasive role in driving |

| | | |
|---|---|---|
| (23273897) | (human A431 and Hela cell lines) | Arp2/3 complex-mediated actin assembly in cooperation with FAK at invasive cell edges, but WRC depletion can promote 3D cell motility." |
| Snapper 2001 (11584271) | Fibroblasts (MEFs isolated from N-WASP$^{+/+}$ and N-WASP$^{neo/neo}$) | N-WASP is dispensable for spreading and filopodia formation in fibroblasts |
| Mizutani 2002 (11830518) | Fibroblasts (rat) | N-WASP is essential for podosome adhesion structures and degrading extracellular matrix. |